MODELLING BIOLOGICAL MACROMOLECULES IN SOLUTION: THE GENERAL TRI-AXIAL ELLIPSOID

Stephen Ernest Harding, M.A. (Oxon), M.Sc.

PhD Dissertation

University of Leicester

1980

CHAPTER 4

Determination of a Stable, Unique Solution by Combining Results from Viscosity, Sedimentation and Electric Birefringence

4.1 Methods for Analyzing the Decay Curve

Resolution of a 2-term exponential birefringence decay curve into its two component relaxation times or decay constants is notoriously difficult, even for components that differ by several orders of magnitude. The situation is especially difficult for globular macromolecules for which the decay constants will generally not differ by more than ~20% (see below). A recent review of the salient methods currently used for attempting to analyse multi-component exponential decay curves, emphasing these difficulties, has been given by Jost and O'Konski (1978). The three methods that are apparently the most useful are

(1) Graphical Peeling Analysis (O'Konski and Haltner, 1956)

(2) Non-Linear Least Squares Analysis (Wilde, 1964, Powell and Macdonald, 1972, Gill and Murray, 1976)

(3) Fourier Transform Solution of the Laplace Integral Equation (Gardner, Gardner, Laush & Meinke, 1958)

4.1.1. Graphical Peeling Analysis

In this method, the logarithm of the birefringence is plotted as a function of time. For a single term decay this should of course give a straight line. If the plot for a two-term decay can be extended to relatively long times with sufficient signal-to-noise ratio, and if the two terms are not too close, then the limiting slope will give an estimate for the longest relaxation time (or shortest decay constant). This limiting slope can be extrapolated back to zero time and then "subtracted" from the original signal; the slope of the resultant can then be determined and hence the shortest relaxation time found (Figure 39). As might be expected, this method, although rapid, is very approximate and is of little use for resolving relaxation times of the same order of magnitude. However it is still useful for indicating the orders of magnitude of the decay constants which may be used as initial estimates in non-linear least squares iterative procedures.

4.1.2. Non-Linear Least Squares Iterative Analysis

In this method, the weighted sum of the squares of the residuals χ^2 is calculated between a set of experimental data points and the function to be fitted. If x_j represents the value of the j'th experimental point and $\xi_j(X_m)$ the corresponding computer point for a given estimate for the X, the number of independent variables, then we define our 'goodness of fit' parameter, χ^2, by

$$\chi^2 = \sum_{j=1}^{n} \left(\frac{x_j - \xi_j}{\sigma_j} \right)^2 \tag{110}$$

where σ_j is the standard error in the j'th experimental point. The best values of the X_m are such that $\partial\chi^2/\partial X_m = 0$, for all the X_m. For the particular case of electric birefringence, σ_j is approximately constant for all the x_j (although this is not generally true for photon counting – e.g. fluorescence depolarization anisotropy – experiments) and the minimization condition becomes

$$\frac{\partial F}{\partial X_m} = 0 \tag{111}$$

where

$$F = \sum_{j=1}^{n} \{x_j - \xi_j\}^2 \tag{111b}$$

In the case of a two-term birefringence decay, the minimization is said to be 'non-linear' in that the data are to be fitted to a function which is the sum of a product of terms consisting of an adjustable parameter (i.e. a pre-exponential factor) with another function of another adjustable parameter (i.e. a decay constant or relaxation time). In order to evaluate $\partial F/\partial X_m$ for a current estimate for the parameters X_m, the solution either has to be linearized using a Taylor expansion as outlined by Jost & O'Konski, or alternatively, a quadratic or quasi-Newtonian procedure can be employed (Gill & Murray, 1976). In this latter case, the parameters X_m are iterated until the minimum in F is found. Gill & Murray's algorithm is particularly attractive in that upper and lower limits for the variable can be specified and included as external constraints. A problem with the least squares technique however is that the method is very sensitive to subsidiary minima in χ^2 (or F) leading to false 'best parameters', even for data of very high precision. The presence of these subsidiary minima can often be detected by repeating the analysis for a series of different initial guesses of the adjustable parameters.

4.1.3. Fourier Transform Solution of the Laplace Integral Equation

The birefringence $\Delta n(t) \equiv S(t)$ is written as a Stieljes integral:

$$S(t) = \sum_i^n A_i' e^{-6\theta_i t} \equiv \sum_i^n A_i' e^{-\lambda t} = \int_0^\infty \exp(-\lambda t)\,dh(\lambda) \qquad (112)$$

where h(λ) is a step function, i = +,- and $\lambda = 6\theta_i$.

The right hand side of equation (112) can be rewritten in the form of a Laplace Integral:

$$S(t) = \int_0^\infty \exp(-\lambda t)g(\lambda)d\lambda \tag{113}$$

where $g(\lambda)$ represents a sum of Dirac delta functions. A plot of $g(\lambda)$ versus λ will give a frequency spectrum with peaks; the centre of each peak corresponds to a specific decay constant, and the height of the peak is proportional to the value of the pre-exponential factor A_i. We transform $\lambda = e^{-y}$ and $t = e^x$. Then

$$S(e^x) = \int_{-\infty}^{\infty} \exp[-e^{(x-y)}]g(e^{-y})e^{-y}dy \tag{114}$$

Multiplying by e^x:

$$e^x\, S(e^x) = \int_{-\infty}^{\infty} \exp[-e^{(x-y)}]e^{(x-y)}g(e^{-y})dy \tag{115}$$

Taking the Fourier Transform of the left hand side of (115)

$$F(\mu) = \frac{1}{\sqrt{2\pi}} \int_{-\infty}^{\infty} e^x\, S(e^x)e^{i\mu x}dx \tag{116}$$

Thus

$$F(\mu) = \frac{1}{\sqrt{2\pi}} \int_{-\infty}^{\infty} \left\{ \int_{-\infty}^{\infty} \exp[-e^{(x-y)}]e^{(x-y)}.g(e^{-y})dy \right\} .\exp[i\mu(s + y)]ds \tag{117}$$

with s = x - y. Rearranging

$$F(\mu) = \sqrt{\frac{1}{2\pi}} \int_{-\infty}^{\infty} g(e^{-y})\exp(i\mu y)dy . \int_{-\infty}^{\infty} \exp(-e^{s})e^{s}\exp(i\mu s)ds \tag{118}$$

Now, if we compare equation (113) with equation (114):

$$g(e^{-y})dy \equiv \frac{g(\lambda)}{\lambda} d\lambda \tag{119}$$

Thus if we obtain $g(e^{-y})$ as a function of y, using equation (119) this will be equivalent to a plot of $g(\lambda)/\lambda$ as a function of λ. The right hand side of equation (118) is the product of the Fourier Transform, $G(\mu)$ of $g(e^{-y})$ and the Fourier Transform, $K(\mu)$ of $\exp(-e^{s})$. Therefore

$$F(\mu) = \sqrt{2\pi}\, G(\mu)\; K(\mu) \tag{120}$$

i.e.

$$G(\mu) = \sqrt{\frac{1}{2\pi}}\; \frac{F(\mu)}{K(\mu)} \tag{121}$$

Taking the inverse Fourier Transform of $G(\mu)$:

$$g(e^{-y}) = \frac{1}{2\pi} \int_{-\infty}^{\infty} \frac{F(\mu)}{K(\mu)}\, e^{-iy\mu} d\mu \tag{122}$$

$K(\mu)$ can be evaluated analytically in terms of the complex Γ function:

$$K(\mu) = \sqrt{\frac{1}{2\pi}}\; \Gamma(1 + i\mu) \tag{123}$$

The method therefore has four basic steps:

(i) Evaluate the Fourier Transform of the data (equation 116)

(ii) Divide by the complex Γ function (equation 123)

(iii) $g(e^{-y})$ as a function of y is found by using the inverse Fourier Transform

(iv) A plot of $g(\lambda)/\lambda$ is thus obtained as a function of λ

The advantage of this method is that an initial choice as to the number of exponential terms to be fitted is not required.

4.1.4. Other methods of analysis, previously used for deconvoluting Fluorescence decay curves

O'Connor, Ware and Andre (1979) have recently compared methods for deconvoluting both one and two term exponential fluorescence decay curves (sections 1.5.4, 3.3.2) - methods which could be equally applicable to corresponding birefringence decays. The methods chosen were

(i) Non-Linear Least Squares

(ii) Method of Moments

(iii) Laplace Transforms

(iv) Method of Modulating Functions,

(v) Exponential series method

(vi) Fourier Transforms

They discovered that all six methods were satisfactory for analysing undistorted one - component data, but that the least squares method was most suitable when distortions are present. For resolving two closely spaced terms (9.5ns & 11.5ns) in a 2-term undistorted decay only the least squares method and the method of modulating functions proved satisfactory. They thus concluded that the non-linear least squares iterative method was the technique of preference for the analysis of simple decay laws.

4.2. Choosing the best algorithm: computer simulation

Following the work of Jost & O'Konski (1978) and O'Connor, Ware & Andre (1979), the non-linear least squares iterative and possibly the Fourier Transform Solution of the Laplace Integral Equation methods seemed to be the best available methods for resolving a 2-term exponential birefringence decay. I attempted to test for myself these methods by assuming three proteins of known (tri-axial) dimensions and hence axial ratios (a/b, b/c), assuming a swelling ratio $(\bar{v}_s/\bar{v}) = 1.3$, and $\bar{v} = .73$ (typical for globular proteins). From these values the molecular weight, viscosity increment, R-function, $\delta_{\pm}$ functions, intrinsic viscosity and hence decay constants $\theta_{\pm}$ could be predicted (Table 14). We then assume pre-exponential factors A'_+, A'_-, of, respectively, 0.07 and 0.05 radians taken from a typical initial birefringence $(\equiv A'_+ + A'_-)$ of 0.12 radians (Krause & O'Konski, 1959) and hence the unperturbed decay curve for each simulated protein can be given. The actual individual values for $A'_{\pm}$ are not significant in the analyses, except when they differ by several orders of magnitude (see section 4.5). One then places simulated experimental error on each of 100 data points for the curves, using a computer normal pseudo-random number generator, and, first of all assuming no errors in the molecular weight or intrinsic viscosity, investigate how much error in the data points is tolerable, before each algorithm fails to give back the correct decay constants and hence axial ratios, within reasonable limits. The algorithms would then be tested for errors in the intrinsic viscosity and molecular weight. Figure 40 illustrates such a mock experimental decay curve with 0.1 degree standard error (about the current available experimental precision - B. Jennings & V. Morris, private communication) on each of 1000 data points, for Protein 1 [true (a/b, b/c) = (1.5, 1.5)]. In the analyses the pre-exponential factors $A'_{\pm}$ are of course regarded as unknown variables.

4.3 Non-Linear Least Squares Iterative Method

The quasi-Newtonian quadratic method for minimizing any function (i.e. in this case, the sum of the squares of the residuals F) given by Gill & Murray (1976) and incorporated in the UK NAG Mk.VI subroutine E04JAF was used. In this algorithm the user, besides supplying the subroutine for calculating the value of F at any point X, has to supply fixed upper and lower bounds on the independent variables X_1, X_2, ..., X_m. This routine was incorporated in the FORTRAN IV program given in Appendix IV, as Program 5. This program generated its own hypothetical decay curve with normal (Gaussian) pseudo-random error generated on each data point (using NAG routine G05ADF), the amount specifiable by the user. The program attempted to retrieve the decay constants, hence the $\delta_{\pm}$ functions (from the user-specified molecular weight and intrinsic viscosity) and hence the axial ratios (a/b, b/c) of the general tri-axial ellipsoid. Owing to the problem of the presence of the danger of the routine falling into subsidiary minima as mentioned by Jost & O'Konski (1978) - see section 4.1.2. - it was necessary to repeat the method for a large number (30) of initial guesses. In fact the program was written to generate its own thirty different initial guesses by using "DO" loop between user specifiable initial guess limits.

Unfortunately, even data as accurate as .001 degree standard error on each data point (about 2 orders of magnitude greater than the current experimental precision) failed to give back the correct (a/b, b/c) within reasonable limits, and even data of machine accuracy (14 significant figures) did not generate the exact value of (1.5, 1.5), as Figure 41 illustrates.

4.4. Fourier Transform Solution Method of the Laplace Integral Equation Method

4.4.1. Cut-off Errors

In order to use this method outlined in section 4.1.3., the integrals involved in taking the Fourier Transform of the data (equation 116) and in taking the inverse Fourier Transform (equation 122) have to be solved numerically. Unfortunately, the integrals extended from $-\infty$ to $+\infty$; with real data there exists a finite cut-off time, t_o or equivalently x_o. Cut-off errors tend to increase the height of the error ripples in the final results. For equation (116), if we choose a cut-off too short for μ_o there is a loss of resolution of the component peaks. On the other hand, if we choose a cut-off in μ_o too long then the cut-off at x_o causes the amplitude of the error ripples to increase; μ_o has to be varied therefore to obtain the optimum resolution for a given data set.

4.4.2. Numerical Integration

Following Gardner et al (1958), each value of S(t) was multiplied by the current value of t to give $e^x S(e^x)$ (equation 115). Whereas t ranges from $0 \to \infty$, x ranges from $-\infty$ to $+\infty$, thus we can split the integral in equation (116) into symmetric and anti-symmetric parts:

$$F(\mu) = \sqrt{\frac{1}{2\pi}} \int_{0}^{x_o} [S^*(x) + S^*(-x)]e^{i\mu x}dx \tag{124}$$

Therefore

$$F(\mu) = \sqrt{\frac{1}{2\pi}} \int_{0}^{x_o} \{[S^*(x) + S^*(-x)]\cos \mu x$$

$$+ i[S^*(x) - S^*(-x)]\sin \mu x \} dx \tag{125}$$

giving real and imaginary parts for $F(\mu)$, i.e., F_c & F_s. $K(\mu)$ can be similarly split into real & imaginary parts K_c & K_s. Equation (121) thus becomes:

$$G(\mu) = \sqrt{\frac{1}{2\pi}} \frac{F_c + iF_s}{K_c + iK_s} = \frac{(F_i + iF_s)(K_c - iK_s)}{K_c^2 + K_s^2} \tag{126}$$

and the inverse transform (122) becomes

$$g(e^{-y}) = \frac{1}{2\pi} \int_{-\mu_o}^{\mu_o} \frac{(F_c + iF_s)(K_c + iK_s)}{K_c^2 + K_s^2} (\cos yu - i\sin y\mu)d\mu \tag{127}$$

where μ_o and $-\mu_o$ are the cut-off values for μ. Since all odd values vanish,

$$g(e^{-y}) = \frac{1}{2\pi} \int_{0}^{\mu_o} \left\{ \frac{F_cK_c + F_sK_s}{K_c + K_s} \cos y\mu + \frac{F_sK_c - F_cK_s}{K_c + K_s} \sin y\mu \right\} d\mu \tag{128}$$

The numerical integrations (125) and (128) are solved using the NAG routine D01GAF. The value of the complex Γ function needed for calculating K_c and K_s was deduced using a routine given by Lucas & Terril (1970). As with the non-linear least squares iterative method, the program (Appendix IV Program 6) generated its own synthetic data using NAG normal pseudo-random number routines G05ADF & G05BBF.

4.4.3. Results

The program was firstly checked by applying it to the case first considered by Gardner et al for a single exponential decay, viz.

$$S(t) = 100\ e^{-0.02t}$$

assuming data of machine accuracy (i.e. no perturbation routine included). The retrieved λ from Figure 42 is .021, in close agreement with Gardner et als value. The data was taken at logarithmic intervals (corresponding to equal linear intervals in x). The algorithm was then applied to the two term exponential decay curve for Protein 2. However, even with data of machine accuracy and taken at logarithmic intervals in t (impossible to obtain in practice for our particular case) the retrieved values for λ_i and hence the decay constants was poor and varied with the cut-off values for μ_o as Figure 43 and Table 15 shows. When normal pseudo-random error of .001 deg was applied to the data points, no resolution was possible for all values of μ_o, as Figure 44 clearly demonstrates. We thus conclude this method to be of little use for our case of interest.

4.5. A new R-Constrained Non-Linear Least Squares Algorithm

Owing to the inadequacy of the other treatments for resolving a two-term exponential birefringence decay into its component relaxation times (or decay constants), particularly for globular proteins (close decay constants), I have now developed a new R-constrained least squares algorithm. If the R-function line solution (3.3.1), which can be found from the ratio of the sedimentation regression coefficient k_s to the intrinsic viscosity $[\eta]$, is included in the least squares algorithm (4.3) as a constraint, then the problem is effectively reduced from one of four independent variables (θ_+, θ_-, A'_+, A'_-) to one of three (a/b, A'_+, A'_-). The solution is constrained to lie on the R-curve, thus a given estimate for a/b will necessarily give a 'constrained' value for b/c; the computer program can then calculate the values for δ_+ and δ_- corresponding to this estimate, hence the decay constants (using also the values for $[\eta]$, M_r - equation 107), the decay curve and finally the sum of the squares of the residuals (SSR) between the computer points and the experimental curve. By iterating along this R-curve for a/b and the two pre-exponential factors $A'_{\pm}$, the best estimate for (a/b, b/c) can be found from the minimum value of the SSR.

The constraint of the R-curve was included in the algorithm (Program 7 of Appendix IV) for the three simulated proteins considered previously by use of the Leicester University Computer Library routine E01LF1, a listing of which is given towards the end of Program 7. The user specifies the coordinates of knots in the curve (see Figures 45, 46 & 47), or alternatively, the whole curve digitised, and the routine interpolates between these points using a cubic polynomial ('spline') fit (K. Brodlie, private communication). In the main program, normal (Gaussian) random error of 0.1 degrees on each of the 100 linearly separated data points was supplied using the pseudo random number routines mentioned previously. The magnitude of this error corresponds to that expected from current experimental precision (B.R. Jennings, V. Morris, private communication). It was found in pilot runs that the danger of the algorithm falling into subsidiary minima, as present for the unconstrained case (section 4.3.) was no longer significant. The number of initial guesses was thus reduced from thirty to three to save on Computer time; the best estimates were generally the same for all three initial guesses (except those marked with an asterisk in Tables 16, 17 & 18). The values for (a/b, b/c) retrieved did however depend on the cut-off time specified for the decay curve. If there were no error in the data points then very long cut-off times would be desirable, since this region is dominated by the longest relaxation time (or shortest decay constant, Θ_-). However, the effect of a given absolute error is more pronounced the lower the birefringence signal.

The optimum cut-off time, and hence the best value for (a/b, b/c) was found by repeating for eight different streams of normal random data, specified by the UK NAG Mk VI routine G05BAF(0.N), where N represents the stream number of the random data; the optimum cut-off time for each decay curve was then determined by finding the best standard deviation of the a/b's from the eight streams for increments of 5ns in the cut-off times. The values for the corresponding best mean value for a/b (and hence b/c) together with the corresponding standard error for the eight streams of data could then be found (Tables 16a, 17a & 18a).

This procedure was then repeated allowing for ±1% experimental error in the R-curves (Tables 16b,c, 17b,c, 18b,c). If the points corresponding to $<(a/b, b/c)> +\sigma_E$ are joined together for each of the R-curves, and then those of the $<(a/b, b/c)> -\sigma_E$, regions of allowed values for (a/b, b/c) could then be found (Figures 48, 49 & 50). The mean values agree very closely with the true values (Table 19). The algorithm was then tested for the effect of experimental errors in the intrinsic viscosity (± 1%) and molecular weight (±1.4%). These were found to be not significant (Table 20); indeed, the molecular weight can now be found precisely from the results of sequence analyses. Finally, the algorithm was tested for different initially assumed values for the pre-exponential factors A'_+ and A'_- (Table 21). Again, these were found to have no significant effect on the results; even for pre-exponential factors differing by two orders of magnitude, though the retrieved A'_- was poor, the retrieved a/b was in close agreement with the other values.

Once the value for the axial ratios (a/b, b/c) has been found for a particular protein, it can be combined with the swollen volume of the protein, if known, to determine the axial dimensions. In Table 22 a "model dependent" (section 1.7.1) estimate for V_e has been found for each of the three simulated proteins we have considered by back substitution of the mean values of (a/b, b/c) determined from the analysis above into equation (8) for the viscosity increment, and again the agreement with the initially assumed values (Table 19) is excellent. If the model dependent values of V_e are then combined with the values for (a/b, b/c), the semi-axial dimensions a,b,c for the three proteins considered are found to be (Å):

Protein 1: 45.00, 29.98, 20.01 (45.0, 30.0, 20.0)

Protein 2: 42.28, 25.59, 19.61 (42.5, 25.0, 20.0)

Protein 3: 43.11, 33.58, 19.81 (42.5, 34.0, 20.0)

again, in excellent agreement with the initially assumed (bracketed) values.

4.6. Some Practical Points

In applying these equations and algorithms to real protein and other macromolecular solutions several important factors must be taken into consideration:

(1) Two or more decay constants can also arise if the system is polydisperse. It is therefore essential that the solution be rendered monodisperse by, for example, gel filtration techniques.

(2) It has now been well established that the single exponential decay constant previously resovable from the birefringence decay of monodisperse protein solutions shows a concentration dependence (Riddiford & Jennings, 1967), and it was therefore necessary to determine its value at several concentrations and then extrapolate to infinite dilution. One must naturally assume therefore that the two decay constants for the decay of a monodisperse solution of asymmetric ellipsoids also show a concentration dependence, and hence must be extrapolated to infinite dilution. On the other hand, because of the constraint in our algorithm that they must correspond to δ_+ and δ_-line solutions that intersect with the R-curve, the values for the decay constants are such that they are not the 'true' decay constants for each particular concentration but are closer to the infinite dilution values. Since the extrapolation procedure must therefore be empirical the best estimates for a/b at particular solute concentrations rather than these 'damped' decay constants may be extrapolated to infinite dilution; once the extrapolated value for a/b has been found the corresponding value for b/c can thus also be found from the R-curve.

(3) The requirement on the precision of the electric birefringence apparatus is not only in producing transient decays to a precision of 0.1 degree on each data point but also the availability of response times (i.e. the finite time it takes for the orienting electric pulse to be switched off) of about

an order of magnitude less than that of the faster relaxation time Adequate response times are now available (Williams, Ham & Wright, 1976) however with apparatus that uses a laser light source, cable discharge generator and a memory oscilloscope, giving a response time of ~ 5ns.

(4) In the above analysis it has been shown that greater accuracies in obtaining the axial ratios can be obtained if the optimum cut-off time for the decay is found. In our simulations this was achieved by averaging over several streams of random data; this corresponds in practice to taking several decays of the same preparation. Different samples of the same preparation should be used because of the danger of denaturing the protein by continually pulsing through high electric fields (temperature effects).

(5) It has also been assumed that the R function can be measured to a precision of ~ ±1%. Since s_c values in an s_c versus concentration plot can be determined to within ~ ±.2%(Squire, 1978), the k_s value can presumably be measured to within ±1% (as, from equation 58, it is approximately a function of $(s_c/s) \times \text{concentration}^{-1}$). The intrinsic viscosity $[\eta]$ can also be measured to within ~±1%, the limiting factor here being the accuracy to which the flow times can be measured. The error in R will thus be of the order of 1% after taking into consideration that any systematic errors in measuring absolute solute concentrations will cancel in the ratio $k_s/[\eta]$ (Rowe, 1977).

(6) Finally, it should be pointed out that because of polarisation effects on the electrodes and also the danger of denaturation due to heating effects mentioned in (4), solutions of low ionic strength (<0.01M) generally have to be used. This apparently prevents the investigation of less soluble materials. On the other hand, an interesting new method is being developed

at Brunel University by Professor B. Jennings and his co-workers in which an ultrasonic field rather than an electric field is used to initially orient the macromolecules before the decay is observed. This "acoustic birefringence" (Ballinger & Jennings, 1979) method does not suffer from the problems of electrode polarisation and denaturation associated with ionic strengths $> .01M$ for the electric birefringence case, allowing the possibility for the investigation of less soluble materials.

Table 14. Assumed and derived characteristics of three hypothetical globular proteins

Protein	1	2	3
	ASSUMED VALUES		
Characteristic			
a,b,c	45Å,30Å,20Å	42.5Å,25Å,20Å	42.5Å,34Å,20Å
$\bar{v}$	0.730 ml/gm	0.730 ml/gm	0.730 ml/gm
$\bar{v}_s/\bar{v}$	1.3	1.3	1.3
	DERIVED VALUES		
Characteristic			
a/b,b/c	1.50,1.50	1.70,1.25	1.25,1.70
$\bar{v}_s$	0.949 ml/gm	0.949ml/gm	0.949ml/gm
swollen molecular volume $V_e = \frac{4\pi abc}{3}$	$1.1309732\times10^{-19}cm^3$	$0.89011784\times10^{-19}cm^3$	$1.2105602\times10^{-19}cm^3$
Anhydrous molecular volume $V\ (=(\bar{v}/\bar{v}_s)\ V_e)$	$0.8699793\times10^{-19}cm^3$	$0.684706\times10^{-19}cm^3$	$0.9312001\times10^{-19}cm^3$
Molecular weight $M_r\ (=(N_A/\bar{v})\ V)$	71,744	56,510	76,853
ν	2.892	2.870	2.840
$[\eta]\ (=N_A V_e \nu/M_r)$	2.75 ml/gm	2.72 ml/gm	2.695 ml/gm
R	1.479	1.482	1.496
θ_+^{red} , θ_-^{red}	0.163, 0.116	0.171, 0.115	0.155, 0.125
δ_+ , δ_-	2.821, 2.016	2.943, 1.982	2.645, 2.125
Decay constants* $\theta_\pm = \frac{N_A kT}{6\eta_0\ [\eta] M_r}\ \delta_\pm$	$5.8153835\times10^6 sec^{-1}$, $4.1564612\times10^6 sec^{-1}$	$7.7660465\times10^6 sec^{-1}$, $5.2290121\times10^6 sec^{-1}$	$5.1872430\times10^6 sec^{-1}$ $4.1674860\times10^6 sec^{-1}$
Relaxation times $\tau_\pm = 1/6\theta_\pm$	28.6596ns, 40.0982ns	21.4609ns, 31.8734ns	32.1301ns, 39.9921ns

* T = 293K, η_0 = 0.01 gm cm^{-1} sec^{-1}

Table 15. Retrieved decay constants for varying values of μ_0

	y_1	y_2	$\lambda_1=e^{-y_1}$	$\lambda_2=e^{-y_2}$	$\theta_+ \times 10^{-6} \mathrm{sec}^{-1}$	$\theta_- \times 10^{-6} \mathrm{sec}^{-1}$
11.5	3.13	3.55	0.04372	0.02872	7.286	4.787
11.6	3.00	3.50	0.04979	0.03020	8.292	5.033
11.7	2.94	3.45	0.05287	0.03175	8.811	5.291
12.0	3.14	3.72	0.04328	0.02423	7.214	4.039

True value for $\theta_+ = 7.7660465 \times 10^6 \mathrm{sec}^{-1}$

True value for $\theta_- = 5.2290121 \times 10^6 \mathrm{sec}^{-1}$

Table 16. Determination of the optimum cut-off time for Protein 1.

True (a/b, b/c) = (1.5, 1.5)

(a) No assumed error in R

Cut-off time	80ns	100ns	110ns	115ns	120ns	140ns
	a/b	a/b	a/b	a/b	a/b	a/b
Stream 1	1.580	1.534	1.513	1.503	1.493	1.454
Stream 2	1.946*	1.785	1.692	1.654	1.619	1.497
Stream 3	1.591	1.512	1.483	1.468	1.452	1.392
Stream 4	1.644	1.487	1.425	1.396	1.367	1.249
Stream 5	1.623	1.480	1.426	1.401	1.377	1.287
Stream 6	1.186	1.275	1.303	1.315	1.326	1.364
Stream 7	1.573	1.645	1.678	1.694	1.710	1.772
Stream 8	1.716	1.623	1.590	1.575	1.562	1.514
Mean	1.6074	1.5426	1.5138	1.5008	1.4883	1.4411
σ (SD)	0.209696	0.148967	0.133899	0.132475	0.134402	0.163491
σ (SE)	0.07414	0.05267	0.04734	0.04684	0.04752	0.05780

σ(SD) = Standard Deviation ; σ(SE) = Standard Error

* different answers for different initial guesses

Optimum cut-off time = 115ns

Best estimate for a/b = 1.501 (± .047)

Corresponding estimate for b/c = 1.498

(b) +1% assumed measured error in R

Cut-off time	110ns a/b	115ns a/b	120ns a/b	125ns a/b	130ns a/b	135ns a/b	140ns a/b
Stream 1	1.546	1.534	1.523	1.511	1.500	1.489	1.478
Stream 2	1.837	1.735	1.679	1.633	1.594	1.557	1.522
Stream 3	1.510	1.492	1.474	1.457	1.440	1.423	1.406
Stream 4	1.439	1.406	1.374	1.342	1.310	1.278	1.244
Stream 5	1.442	1.414	1.387	1.361	1.337	1.312	1.289
Stream 6	1.312	1.325	1.340	1.349	1.360	1.370	1.380
Stream 7	1.816	1.871	1.847	1.840	1.878	1.893	1.909
Stream 8	1.643	1.624	1.606	1.590	1.575	1.561	1.548
Mean	1.5681	1.5501	1.5288	1.5104	1.4992	1.4854	1.4720
σ (SD)	0.185700	0.183700	0.174243	0.173033	0.186398	0.195406	0.206181
σ (SE)	0.06565	0.06495	0.06160	0.06118	0.06590	0.06909	0.07290

Optimum cut-off time = 125ns

Best estimate for a/b = 1.510 (± .061)

Corresponding estimate for b/c = 1.400

(c) -1% assumed measured error in R

Cut-off time	110ns a/b	115ns a/b	120ns a/b
Stream 1	1.494	1.485	1.476
Stream 2	1.644	1.616	1.588
Stream 3	1.468	1.454	1.440
Stream 4	1.419	1.392	1.366
Stream 5	1.418	1.395	1.373
Stream 6	1.300	1.311	1.321
Stream 7	1.626	1.638	1.649
Stream 8	1.561	1.549	1.537
Mean	1.4913	1.4800	1.4688
σ (SD)	0.115922	0.114924	0.115761
σ (SE)	0.04098	0.04063	0.04093

Optimum cut-off time = 115ns

Best estimate for a/b = 1.480 (± .041)

Corresponding estimate for b/c = 1.611

Table 17. Determination of the optimum cut-off time for Protein 2.

True (a/b, b/c) = (1.7, 1.25)

(a) No assumed error in R

Cut-off time	85ns a/b	90ns a/b	95ns a/b	100ns a/b	105ns a/b	110ns a/b	120ns a/b
Stream 1	1.709	1.691	1.675	1.659	1.644	1.630	1.603
Stream 2	1.963	1.926	1.872	1.777	1.716	1.666	1.579
Stream 3	1.670	1.645	1.622	1.600	1.578	1.558	1.520
Stream 4	1.602	1.561	1.523	1.486	1.452	1.418	1.351
Stream 5	1.600	1.566	1.534	1.505	1.478	1.453	1.408
Stream 6	1.482	1.496	1.509	1.521	1.533	1.544	1.566
Stream 7	1.924	1.924	1.923	1.923	1.923	1.923	1.922
Stream 8	1.847	1.803	1.771	1.745	1.723	1.703	1.669
Mean	1.7246	1.7015	1.6786	1.6520	1.6309	1.6119	1.5773
σ (SD)	0.170801	0.166408	0.161588	0.154362	0.155373	0.159776	0.173689
σ (SE)	0.06039	0.05883	0.05713	0.05458	0.05493	0.05649	0.06141

Optimum cut-off time = 100ns

Best estimate for a/b = 1.652 (±.055)

Corresponding estimate for b/c = 1.305

(b) <u>+1 % assumed measured error in R</u>

Cut-off time	75ns a/b	80ns a/b	85ns a/b	90ns a/b	95ns a/b	100ns a/b	105ns a/b
Stream 1	1.856	1.856	1.856	1.820	1.821	1.767	1.834
Stream 2	1.856	1.856	1.856	1.856	1.856	1.856	1.856
Stream 3	1.856	1.821	1.791	1.732	1.691	1.658	1.628
Stream 4	1.843	1.728	1.655	1.599	1.551	1.508	1.467
Stream 5	1.834	1.716	1.655	1.608	1.568	1.532	1.501
Stream 6	1.471	1.492	1.511	1.528	1.544	1.560	1.575
Stream 7	1.856	1.856	1.856	1.856	1.856	1.856	1.856
Stream 8	1.856	1.856	1.856	1.856	1.856	1.856	1.856
Mean	1.8035	1.7726	1.7545	1.7319	1.7179	1.6991	1.6841
σ (SD)	0.134604	0.127668	0.131819	0.135561	0.145962	0.153037	0.163378
σ (SE)	0.04759	0.04514	0.04661	0.04791	0.05161	0.05411	0.05776

Optimum cut-off time = 80ns

Best estimate for a/b = 1.773 ($\pm$.045)

Corresponding estimate for b/c = 1.0875

(c) -1% assumed measured error in R

Cut-off time	80ns	85ns	90ns	95ns	100ns	105ns
	a/b	a/b	a/b	a/b	a/b	a/b
Stream 1	1.670	1.656	1.643	1.630	1.617	1.605
Stream 2	1.936†	1.861	1.799	1.749	1.705	1.665
Stream 3	1.648	1.628	1.608	1.589	1.570	1.552
Stream 4	1.614	1.576	1.541	1.507	1.475	1.444
Stream 5	1.606	1.573	1.543	1.516	1.490	1.466
Stream 6	1.452	1.466	1.478	1.489	1.499	1.509
Stream 7	1.815	1.842	1.870	1.902	1.936†	1.936†
Stream 8	1.759	1.737	1.716	1.698	1.681	1.666
Mean	1.6875	1.6674	1.6498	1.6350	1.6216	1.6054
σ (SD)	0.147596	0.137488	0.136111	0.142556	0.153928	0.157728
σ (SE)	0.05218	0.04861	0.04812	0.05040	0.05442	0.05577

† Upper limit ($\equiv b/c = 1.0$)

Optimum cut-off time = 90ns

Best estimate for a/b = 1.650 (± .048)

Corresponding estimate for b/c = 1.3905

Table 18. Determination of the optimum cut-off time for Protein 3.

True (a/b, b/c) = (1.25, 1.7)

(a) No assumed error in R

Cut-off time	80ns	100ns	105ns	110ns	115ns	120ns	140ns
	a/b	a/b	a/b	a/b	a/b	a/b	a/b
Stream 1	1.367	1.315	1.303	1.291	1.278	1.266	1.215
Stream 2	1.881	1.587	1.547	1.510	1.476	1.442	1.313
Stream 3	1.388	1.301	1.281	1.263	1.240	1.219	1.119
Stream 4	1.464	1.285	1.244	1.200	1.151	1.089	1.001
Stream 5	1.448	1.278	1.239	1.200	1.157	1.108	1.000
Stream 6	1.000	1.000	1.000	1.000	1.000	1.000	1.000
Stream 7	1.314	1.393	1.409	1.424	1.439	1.453	1.505
Stream 8	1.514	1.421	1.402	1.385	1.370	1.354	1.297
Mean	1.4220	1.3225	1.3031	1.2841	1.2639	1.2414	1.1813
σ (SD)	0.243637	0.165850	0.160554	0.158626	0.161019	0.168224	0.184692
σ (SE)	0.08614	0.05864	0.05676	0.05608	0.05693	0.05948	0.06530

Optimum cut-off time = 110ns

Best estimate for a/b = 1.284 (± .056)

Corresponding estimate for b/c = 1.695

(b) +1% assumed measured error in R

Cut-off time	105ns a/b	110ns a/b	115ns a/b
Stream 1	1.319	1.306	1.293
Stream 2	1.618	1.562	1.516
Stream 3	1.294	1.272	1.249
Stream 4	1.247	1.199	1.145
Stream 5	1.245	1.202	1.155
Stream 6	1.000	1.000	1.000
Stream 7	1.444	1.462	1.481
Stream 8	1.431	1.412	1.394
Mean	1.3248	1.3019	1.2791
σ (SD)	0.181404	0.176485	0.178272
σ (SE)	0.06414	0.06240	0.06303

Optimum cut-off time = 110ns

Best estimate for a/b = 1.302 (± .062)

Corresponding estimate for b/c = 1.5395

(c) <u>-1% assumed measured error in R</u>

Cut-off time	105ns a/b	110ns a/b	115ns a/b
Stream 1	1.294	1.283	1.271
Stream 2	1.511	1.481	1.452
Stream 3	1.275	1.257	1.238
Stream 4	1.246	1.206	1.163
Stream 5	1.240	1.204	1.165
Stream 6	1.000	1.000	1.000
Stream 7	1.387	1.400	1.413
Stream 8	1.385	1.370	1.355
Mean	1.2923	1.2751	1.2571
σ(SD)	0.149290	0.147794	0.149222
σ(SE)	0.05278	0.05225	0.05276

Optimum cut-off time = 110ns

Best estimate for a/b = 1.275 (± .052)

Corresponding estimate for b/c = 1.764

Table 19. Mean values for the retrieved axial ratios compared with the real values

	Retrieved $(\frac{a}{b}, \frac{b}{c})$	Real $(\frac{a}{b}, \frac{b}{c})$
Protein 1	(1.501, 1.498)	(1.50, 1.50)
Protein 2	(1.652, 1.305)	(1.70, 1.25)
Protein 3	(1.284, 1.695)	(1.25, 1.70)

Table 20. Effect of experimental errors in the intrinsic viscosity and molecular weight

(and hence the product $[\eta] . M_r$ used in calculating the decay constants – cf Table 14 and equation 108)

Assumed error in $[\eta] = \pm 1\%$
" " " $M_r = \pm 1.4\%$
} total error ~ ±1.7 % (calculated from formula given in Paradine & Rivett (1960))

Results are for Protein 1, cut-off time = 115ns, $\pm 0.1^{\circ}$ standard error on each of the 100 data points

Stream no. of random data	– 1.7%	No error a/b	+ 1.7%
1	1.493	1.503	1.520
2	1.638	1.654	1.679
3	1.455	1.468	1.487
4	1.374	1.396	1.424
5	1.383	1.401	1.425
6	1.305	1.315	1.333
7	1.695	1.694	1.704
8	1.566	1.575	1.593
mean a/b	1.4886	1.5008	1.5206
σ_{SD}	0.136305	0.132475	0.130253
σ_{SE}	0.04819	0.04684	0.04668

σ_{SD} = standard deviation

σ_{SE} = standard error

Table 21. Effect of using different initially assumed values for the pre-exponential factors $A'_{\pm}$

Protein 1, Cut off time = 100 ns, 0.1 s.e. on each of the 100 data points*

Assumed		Retrieved		
A'_{+}	A'_{-}	a/b	A'_{+}	A'_{-}
0.06	0.06	1.683	0.057	0.064
0.07	0.05	1.674	0.065	0.055
0.09	0.03	1.660	0.083	0.038
0.11	0.01	1.664	0.099	0.021
0.119	0.001	1.644	0.109	0.012

*The data for this table were obtained after the UK NAG Mk VI routines had been updated to Mk VII; the new random number routines corresponding to G05ADF & G05BAF in Mk VI are G05CAF & G05CBF

Table 22. Comparison of model dependent estimates for V_e with the real values

	Retrieved $(\frac{a}{b}, \frac{b}{c})$	Model-dependent* V_e (cm^3)	Real V_e (cm^3) (cf Table 14)
Protein 1	(1.501, 1.498)	1.131×10^{-19}	1.131×10^{-19}
Protein 2	(1.652, 1.305)	0.889×10^{-19}	0.890×10^{-19}
Protein 3	(1.284, 1.695)	1.202×10^{-19}	1.211×10^{-19}

*calculated by determining the value of ν corresponding to $(\frac{a}{b}, \frac{b}{c})$ and then back substituting into the equation $\nu = [\eta]M_r/N_A V_e$, where $[\eta]$ is in ml/gm

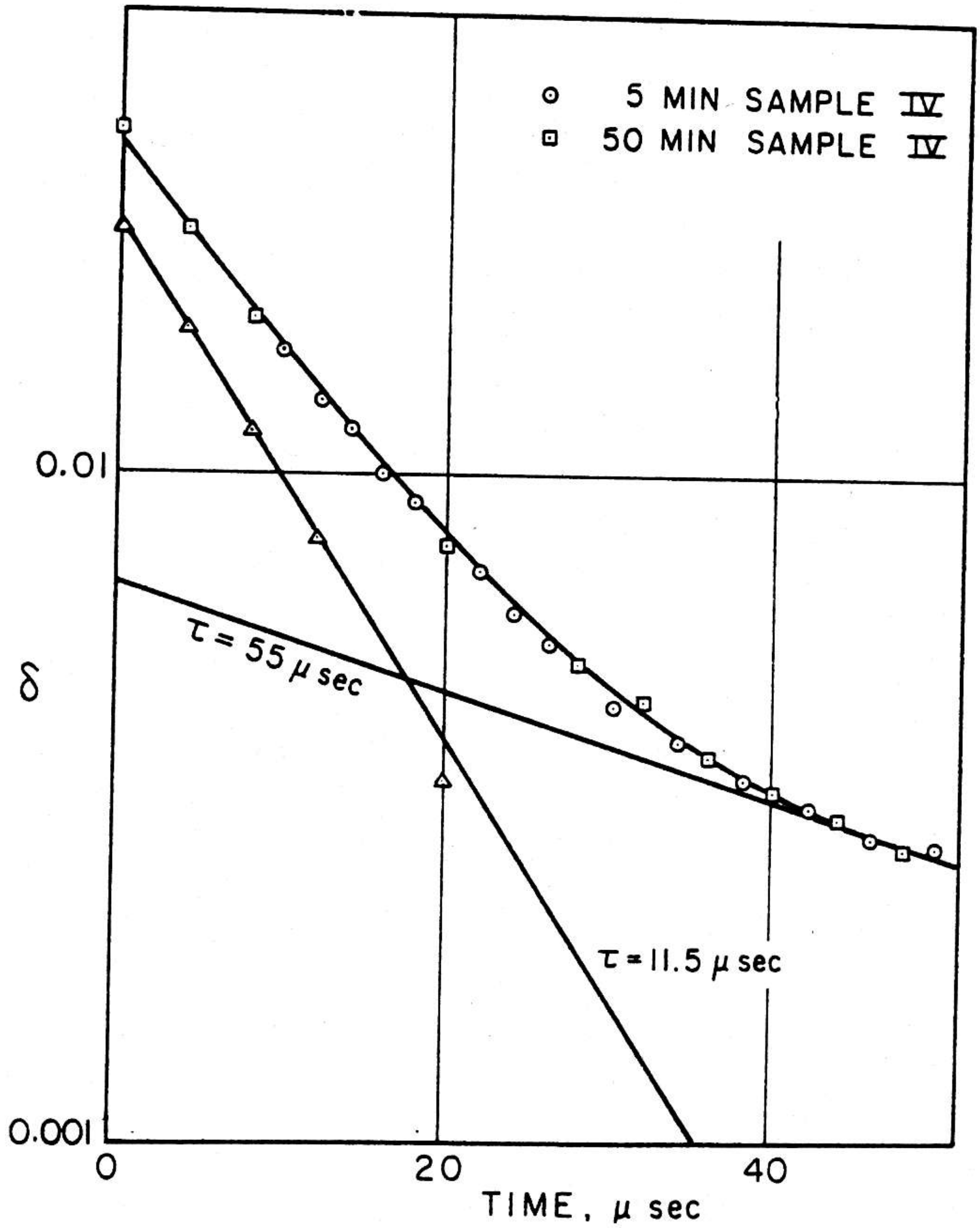

Figure 39. Birefringence decay (expressed in radians) in Helix Pomatia hemocyanin solutions. The triangles represent the difference between the tangential curve (long relaxation time) and the experimental points. (From Pytkowickz & O'Konski, 1959)

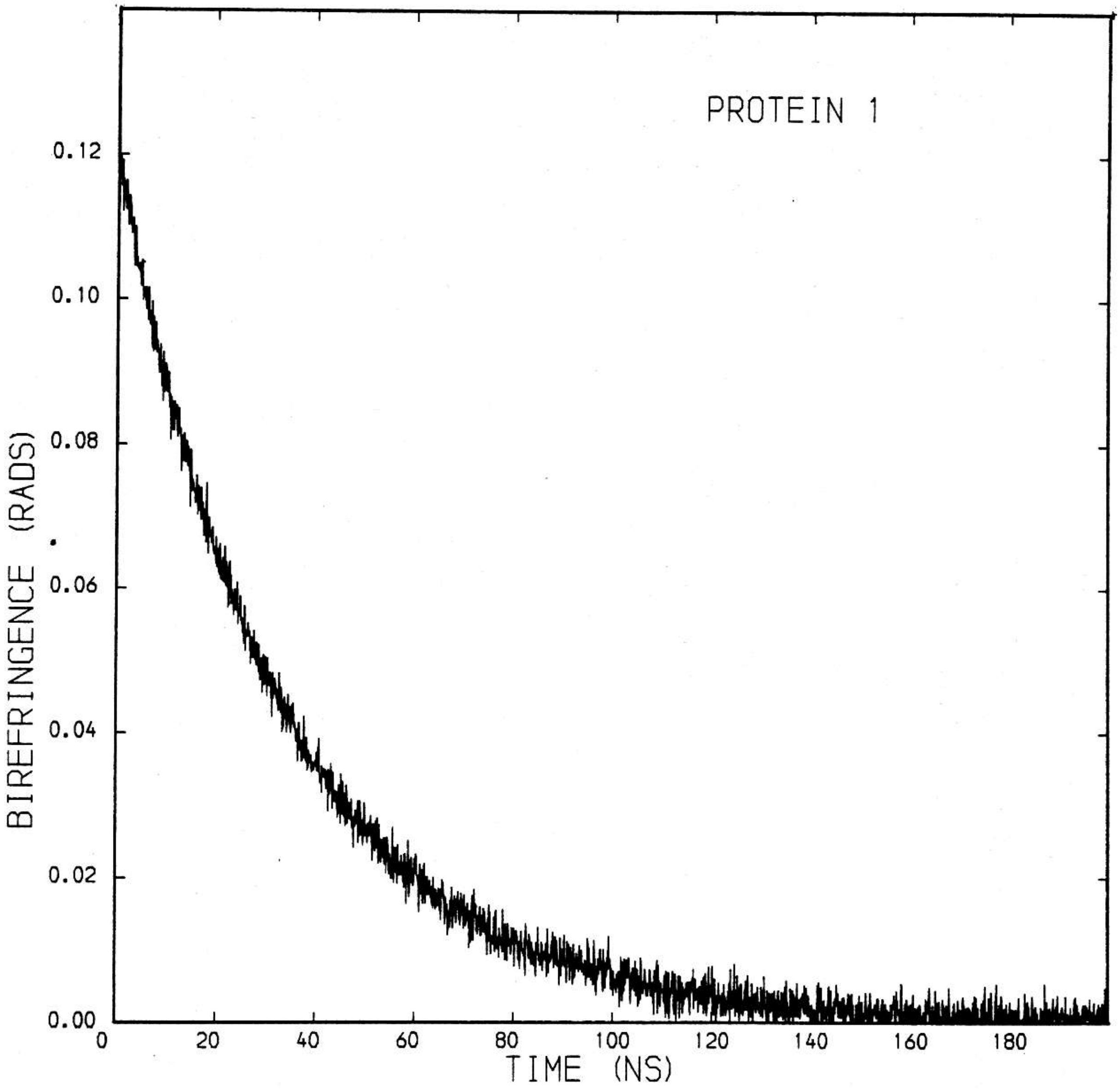

Figure 40. **Synthetic two-term exponential electric birefringence decay curve assuming a standard error of ± 0.1° on each data point.**

Relaxation times assumed: 28.66ns, 40.10ns

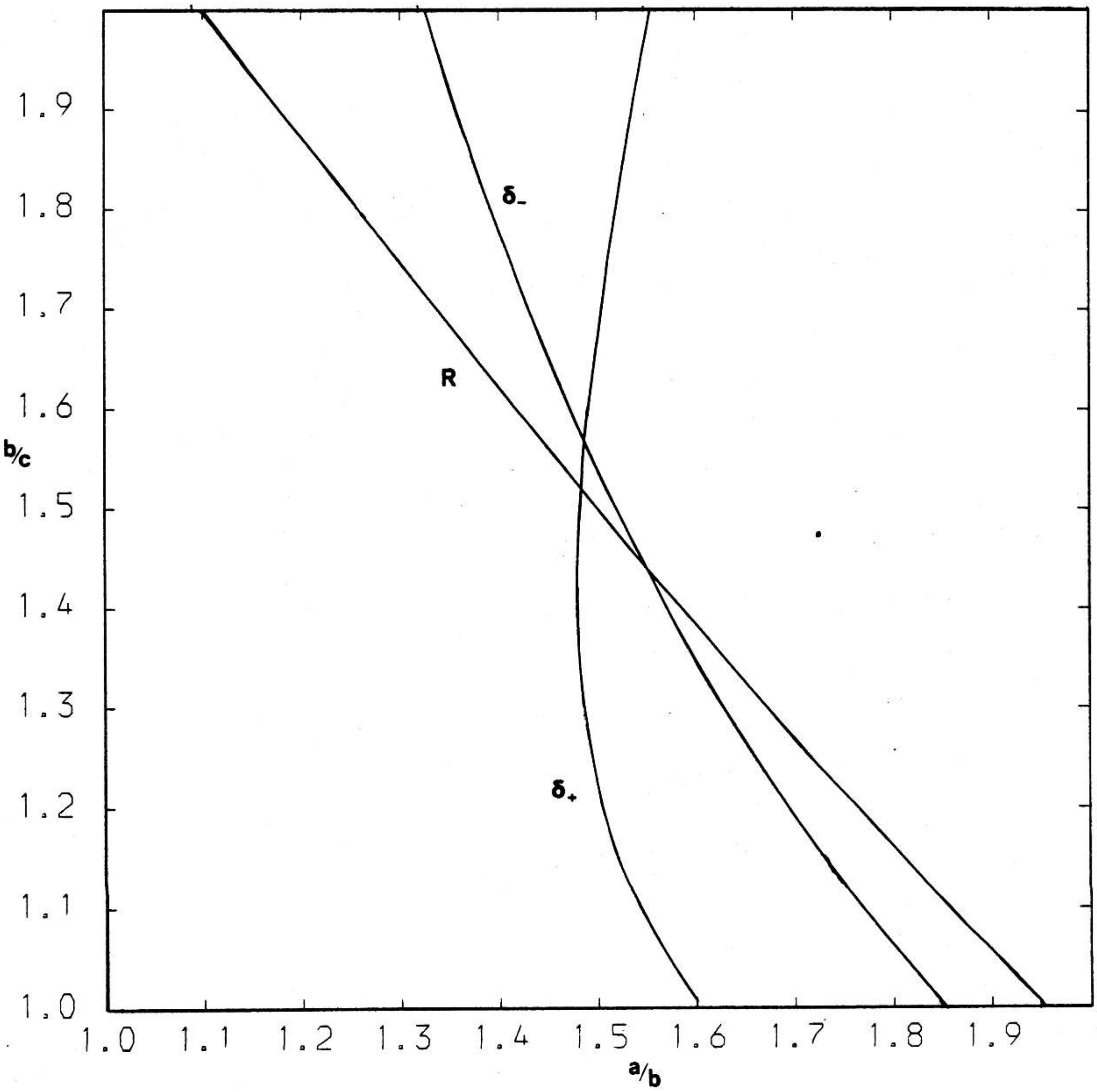

Figure 41. Plot of the R, δ_+ and δ_- values obtained from the non-linear least squares analysis assuming birefringence data of machine accuracy

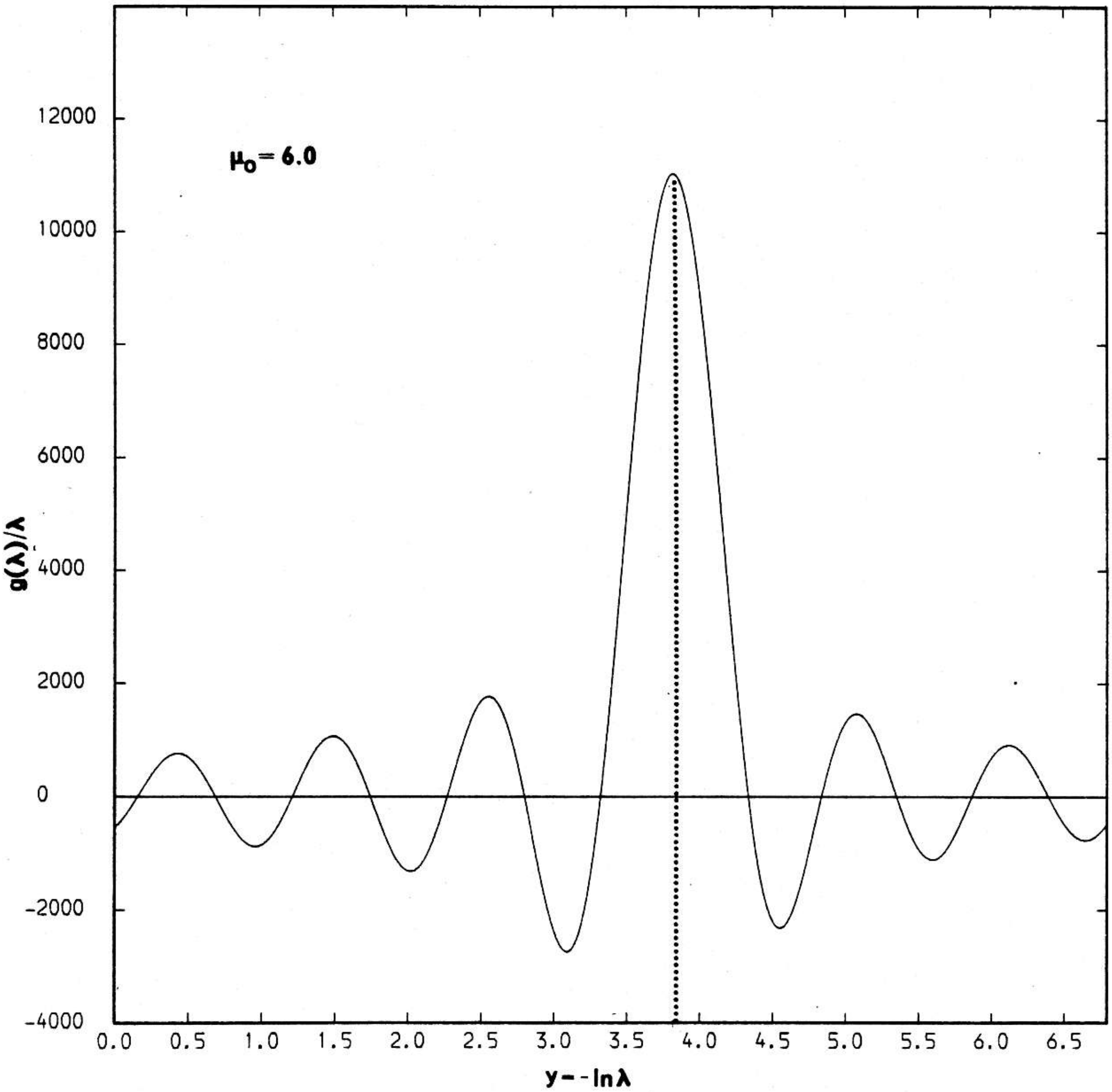

<u>Figure 42</u>. <u>Frequency spectrum of λ ($\equiv$1/relaxation time) for a single exponential decay and μ_o = 6.0, assuming decay data of machine accuracy (14 figures)</u>. The position of the highest peak corresponds to a value of λ of .021, in agreement with the initially assumed value of 0.02

Figure 43 (I - VI)

Effect of increasing μ_0 to determine best resolution of the frequency spectrum corresponding to the decay for Protein 2, for 140 logarithmically increasing data points of machine accuracy (14 figures)

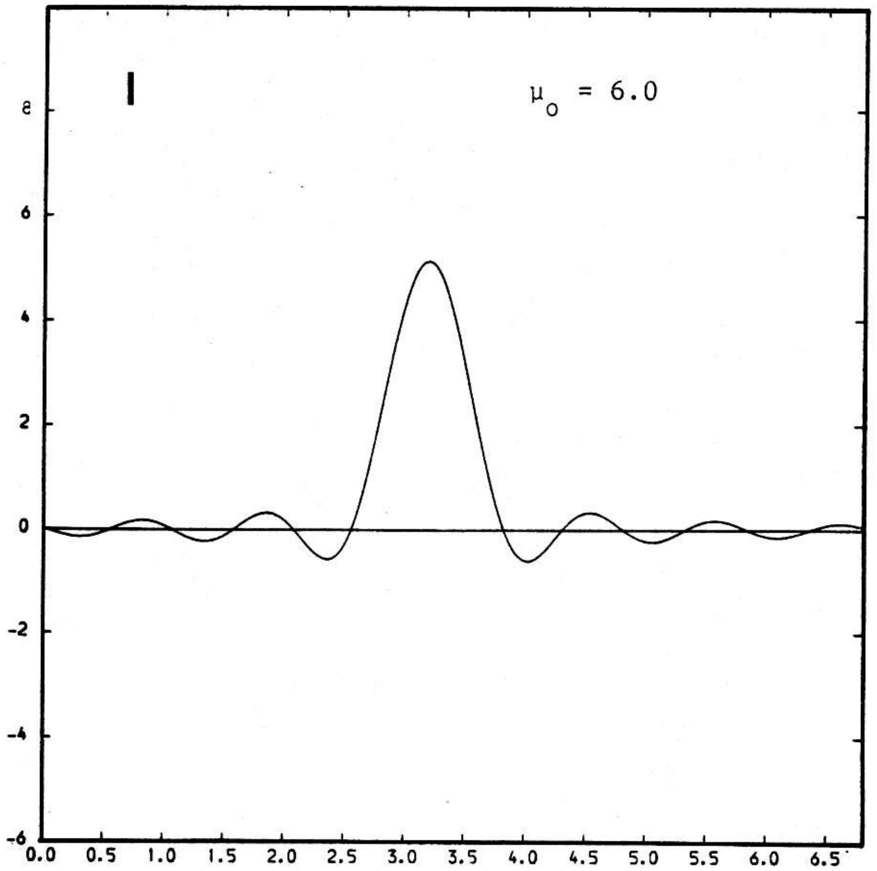
I
μo = 6.0
8
6
4
2
0
-2
-4
-6
0.0 0.5 1.0 1.5 2.0 2.5 3.0 3.5 4.0 4.5 5.0 5.5 6.0 6.5

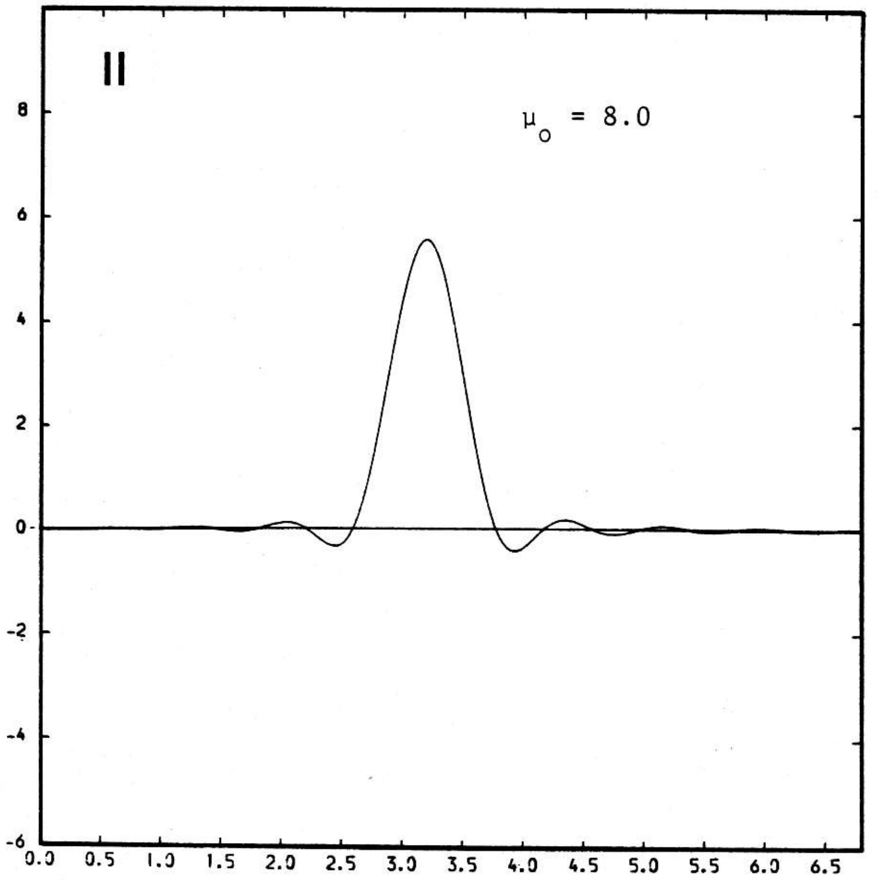
II
μo = 8.0
8
6
4
2
0
-2
-4
-6
0.0 0.5 1.0 1.5 2.0 2.5 3.0 3.5 4.0 4.5 5.0 5.5 6.0 6.5

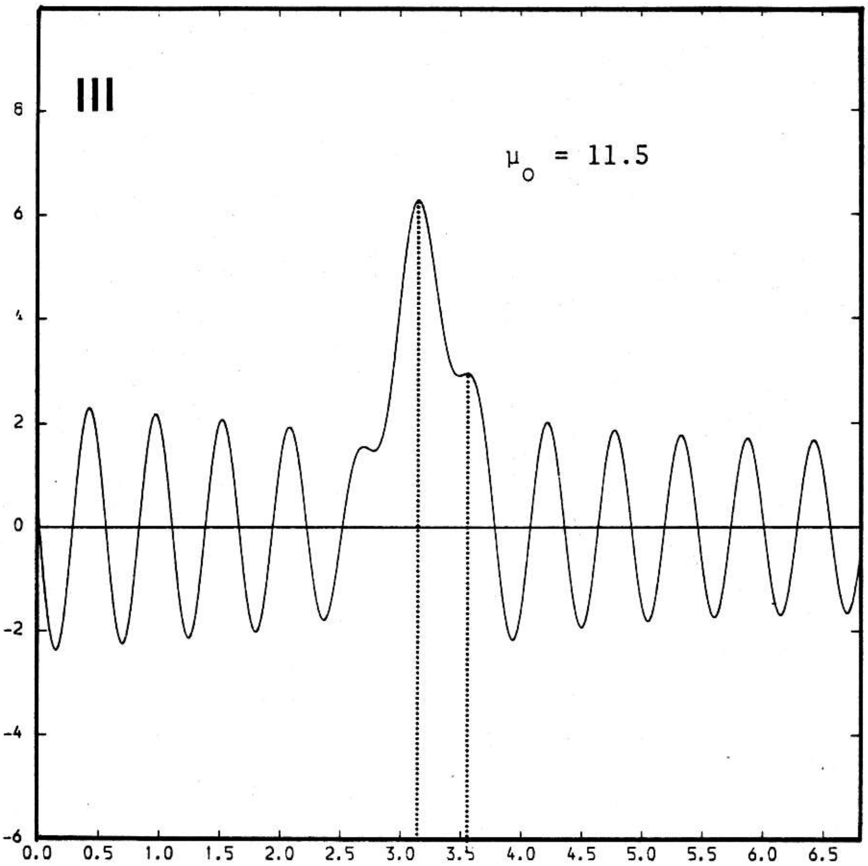
III
μ_O = 11.5
8
6
4
2
0
-2
-4
-6
0.0
0.5
1.0
1.5
2.0
2.5
3.0
3.5
4.0
4.5
5.0
5.5
6.0
6.5

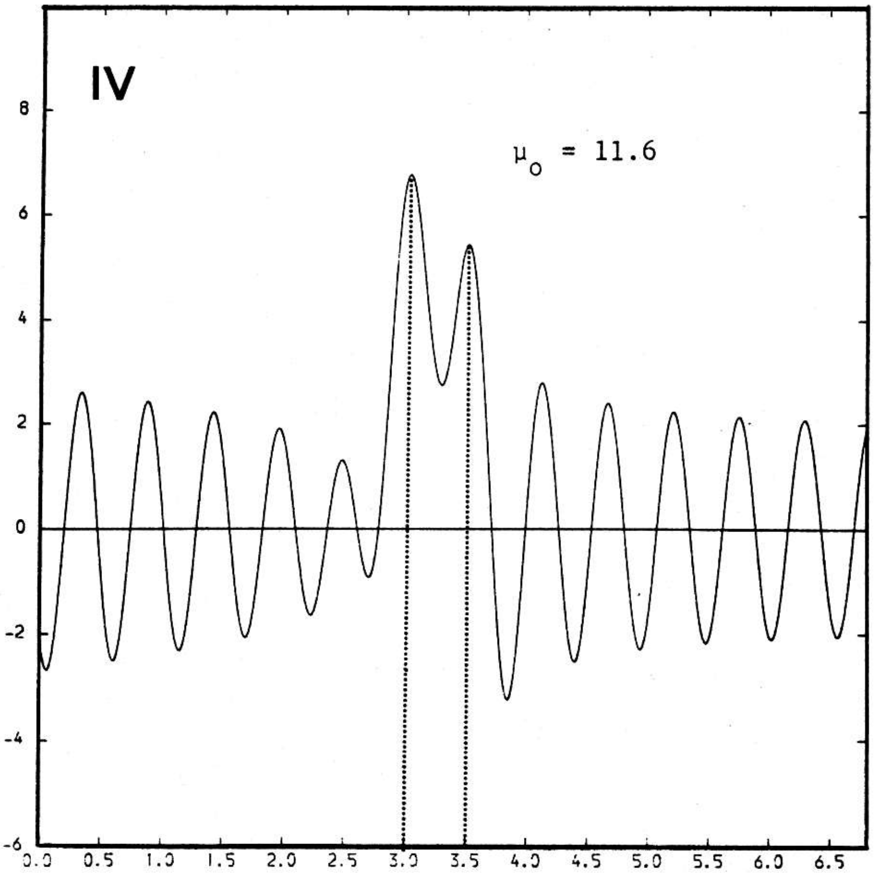
IV
μ_O = 11.6
8
6
4
2
0
-2
-4
-6
0.0
0.5
1.0
1.5
2.0
2.5
3.0
3.5
4.0
4.5
5.0
5.5
6.0
6.5

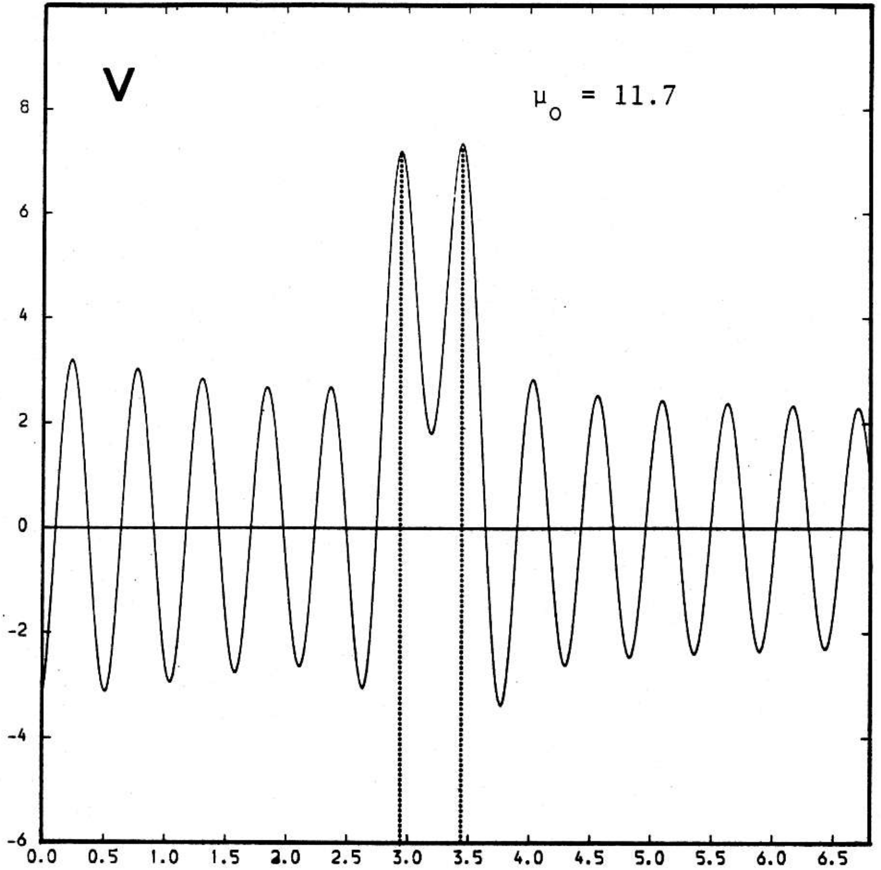
V
μ_o = 11.7
8
6
4
2
0
-2
-4
-6
0.0
0.5
1.0
1.5
2.0
2.5
3.0
3.5
4.0
4.5
5.0
5.5
6.0
6.5

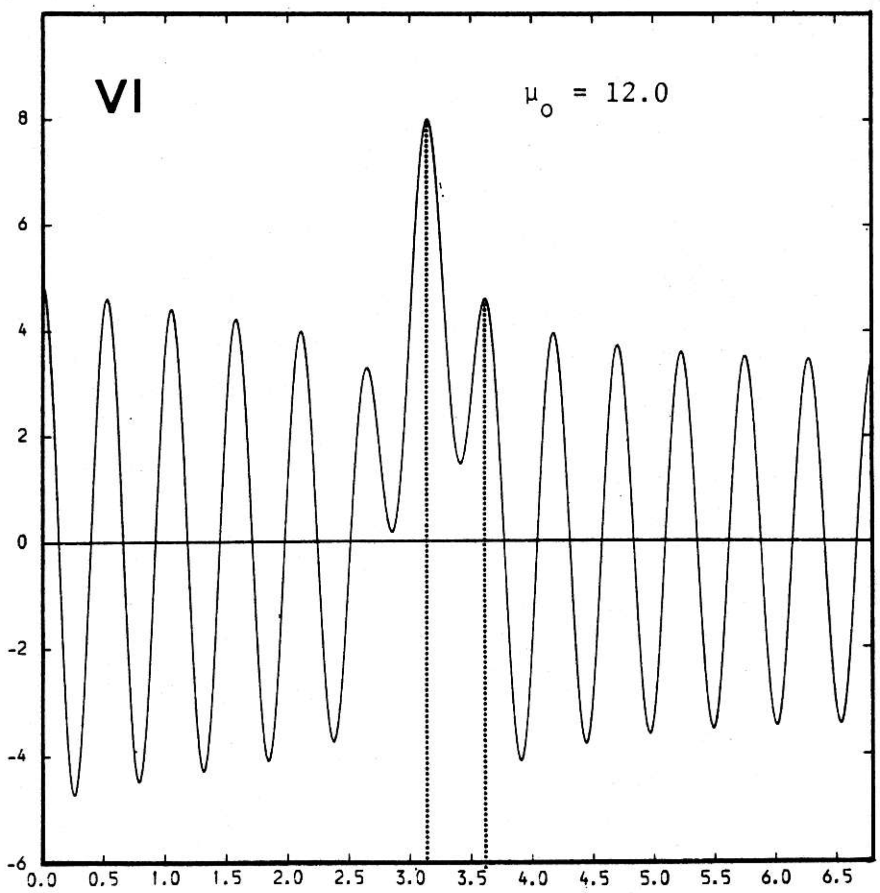
VI
μ_o = 12.0
8
6
4
2
0
-2
-4
-6
0.0
0.5
1.0
1.5
2.0
2.5
3.0
3.5
4.0
4.5
5.0
5.5
6.0
6.5

<u>Figure 44</u> (I - VI)

As for Figure 43 but for data of $.001^{\circ}$ standard error on each of the 140 logarithmically increasing data points

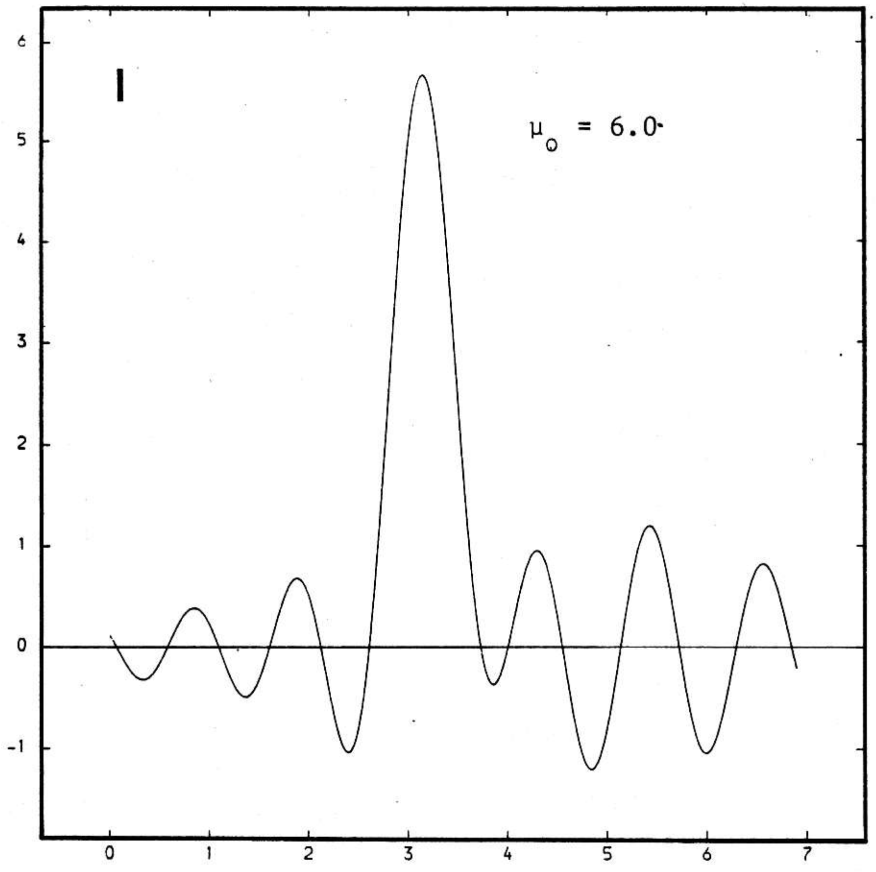
I
μ_o = 6.0
6
5
4
3
2
1
0
-1
0
1
2
3
4
5
6
7

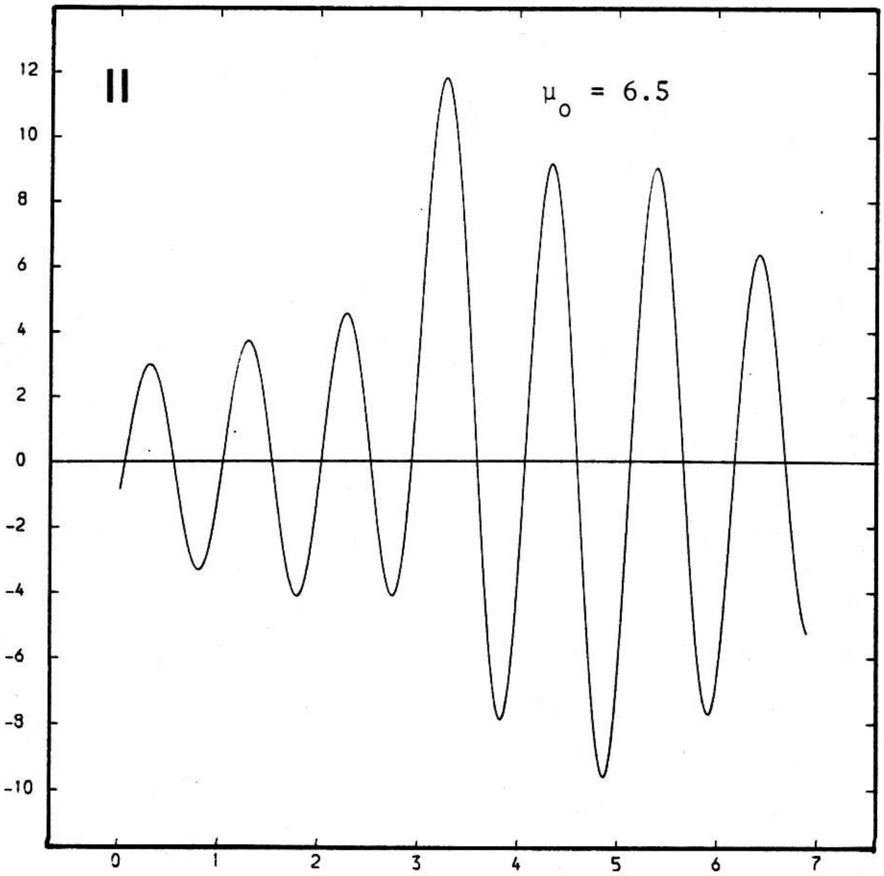
II
μ_o = 6.5
12
10
8
6
4
2
0
-2
-4
-6
-8
-10
0
1
2
3
4
5
6
7

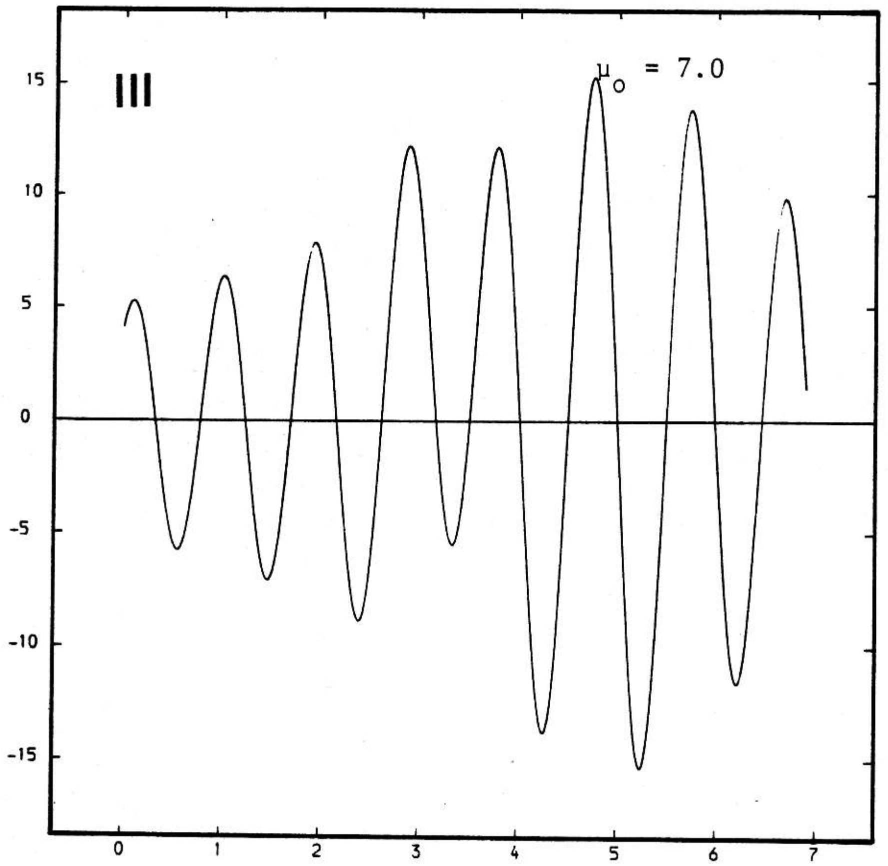
III
μ_o = 7.0
15
10
5
0
-5
-10
-15
0
1
2
3
4
5
6
7

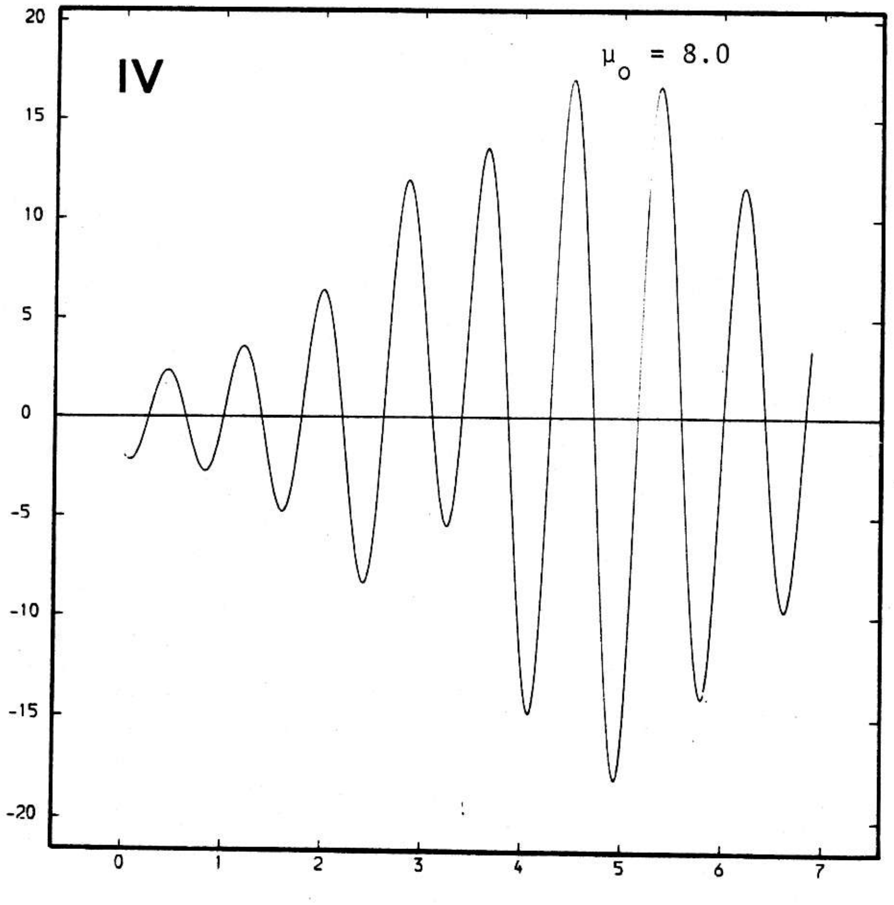
IV
μ_o = 8.0
20
15
10
5
0
-5
-10
-15
-20
0
1
2
3
4
5
6
7

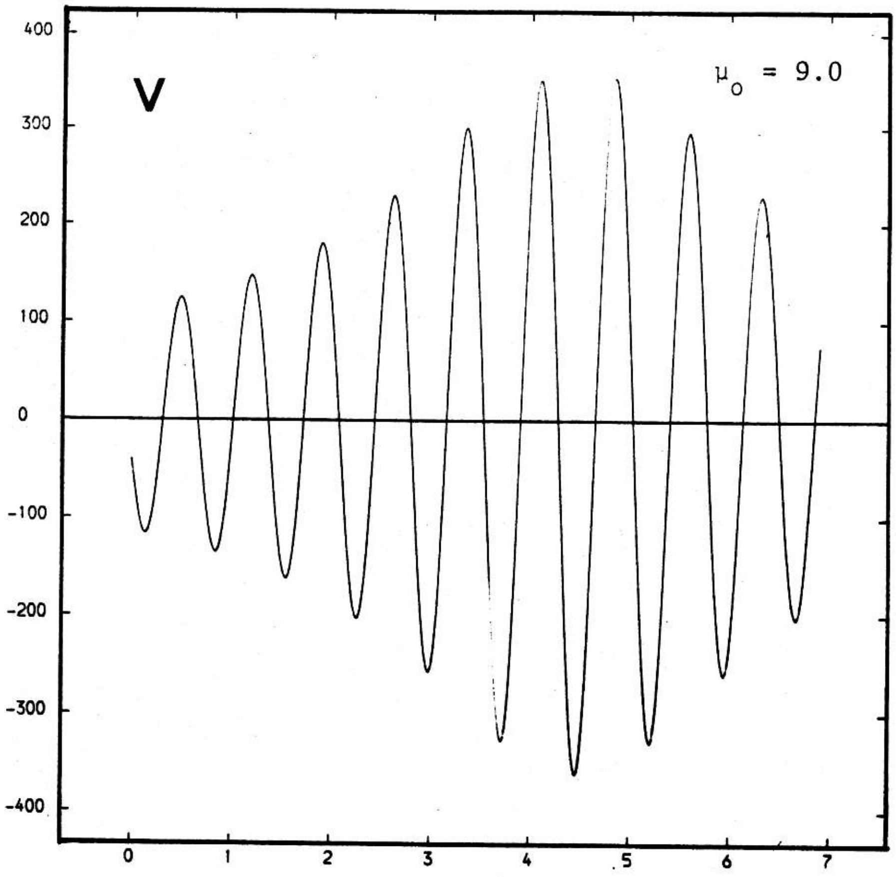
V
μ_o = 9.0
400
300
200
100
0
-100
-200
-300
-400
0
1
2
3
4
5
6
7

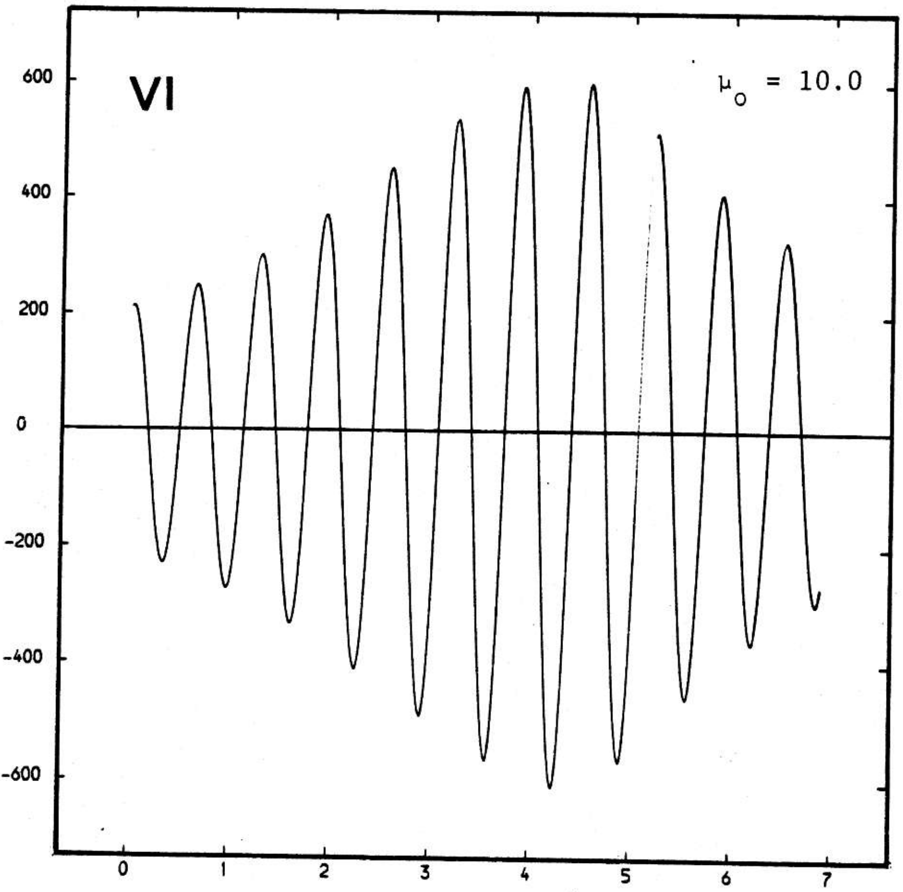
VI
μ_o = 10.0
600
400
200
0
-200
-400
-600
0
1
2
3
4
5
6
7

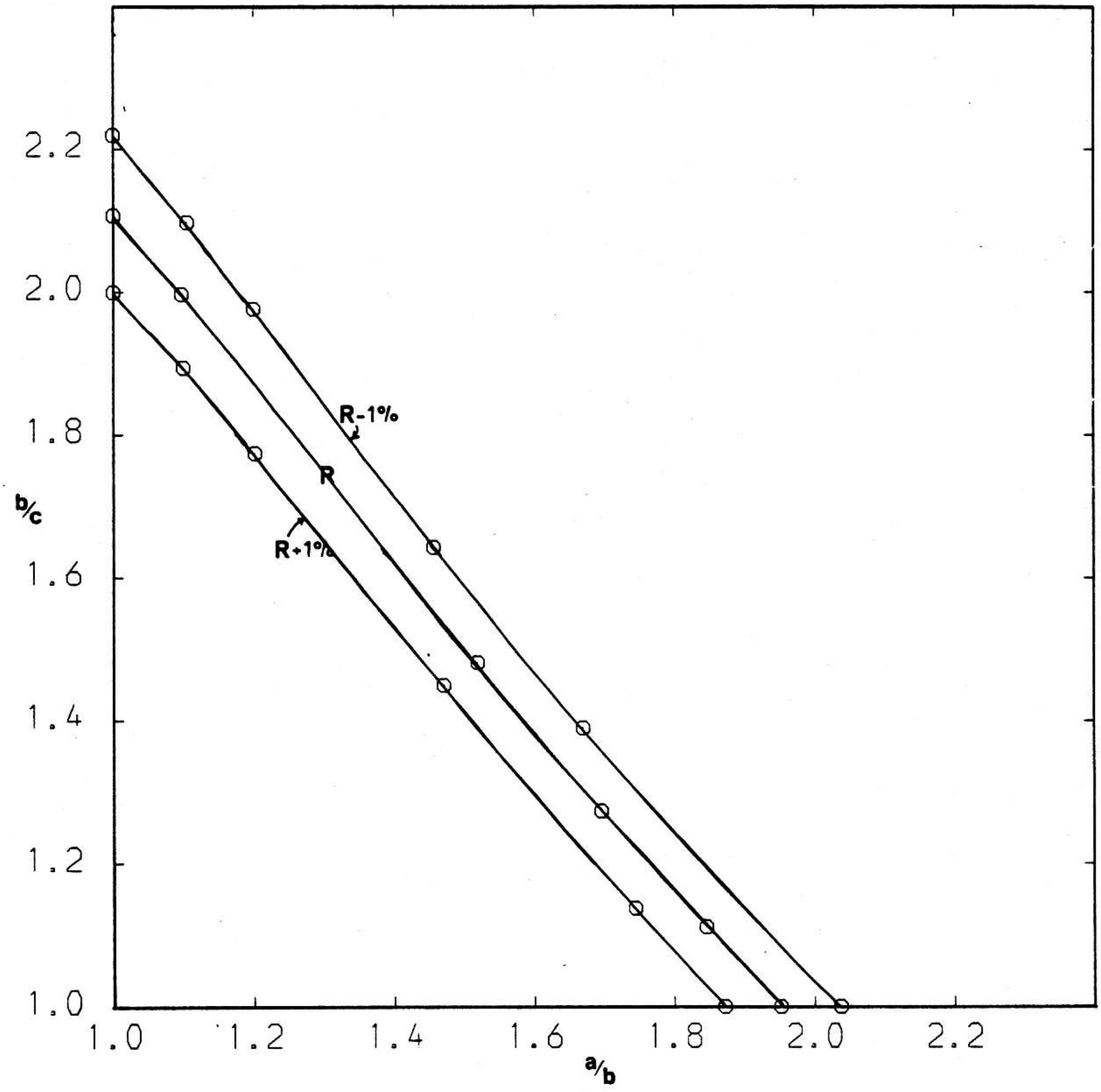

Figure 45. Knots in the R curves for specification in the R – constrained least squares analysis (Program 7) for Protein 1

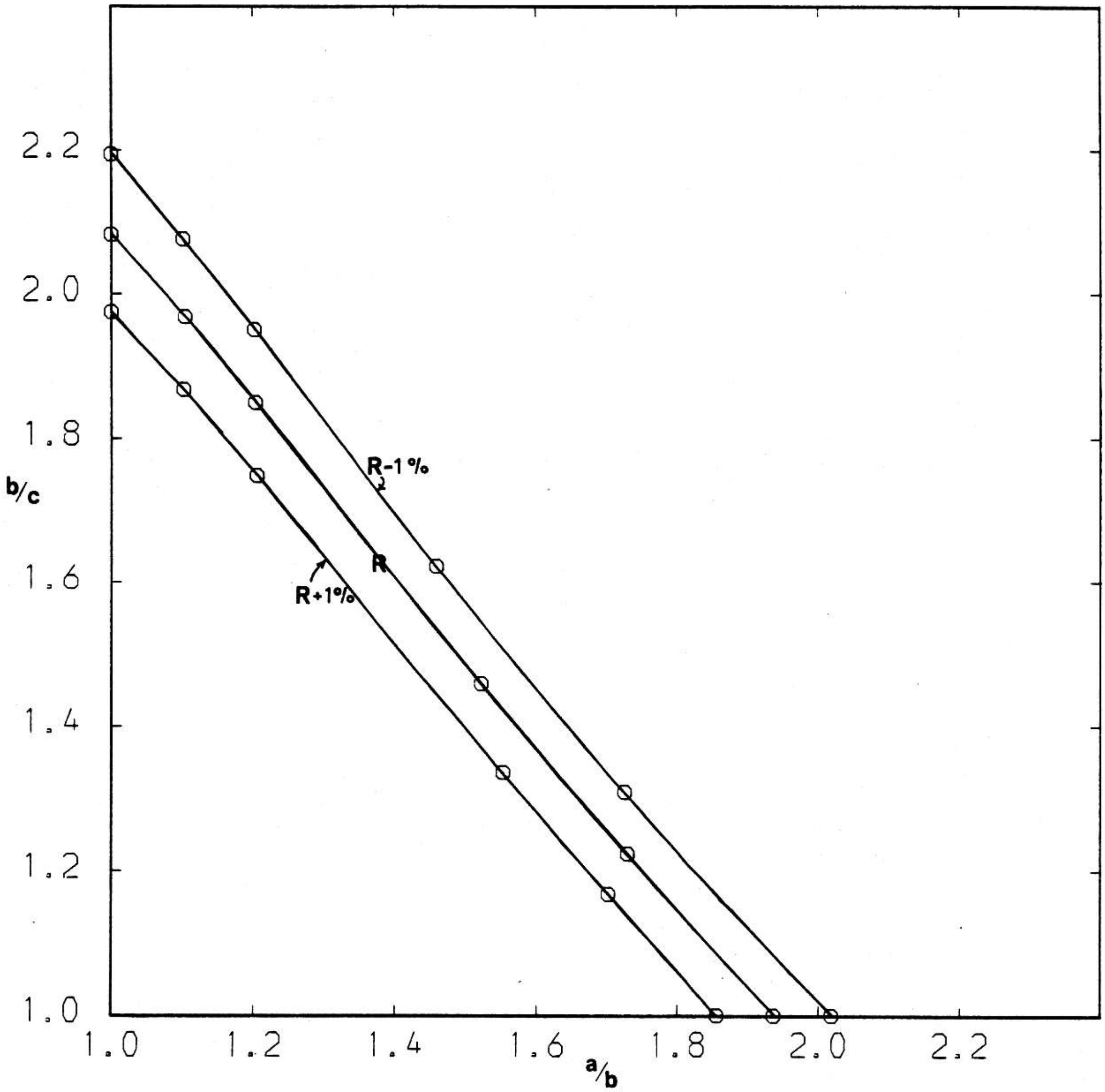

Figure 46. As for Figure 45 but for Protein 2

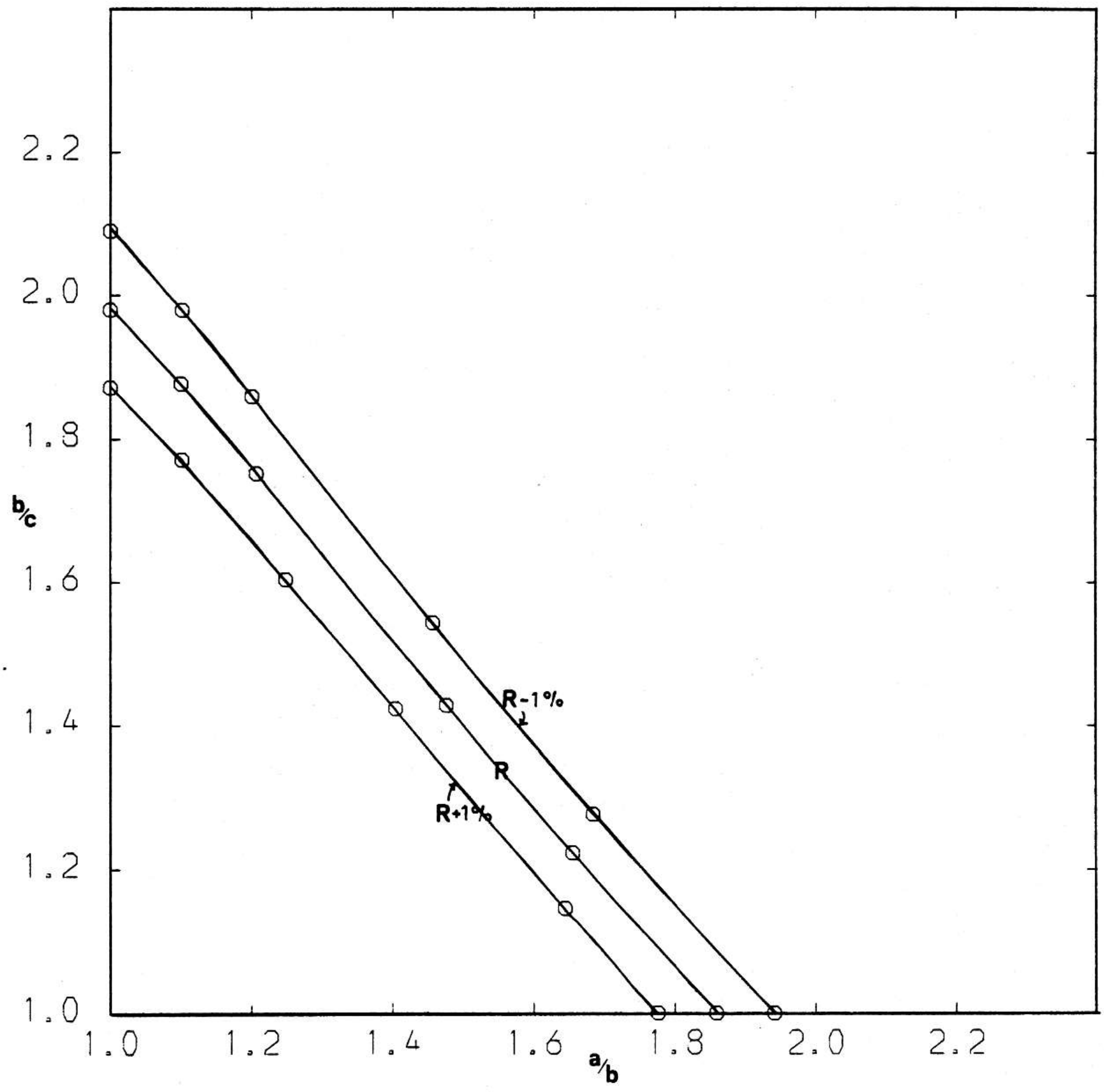

Figure 47. As for Figure 45 but for Protein 3

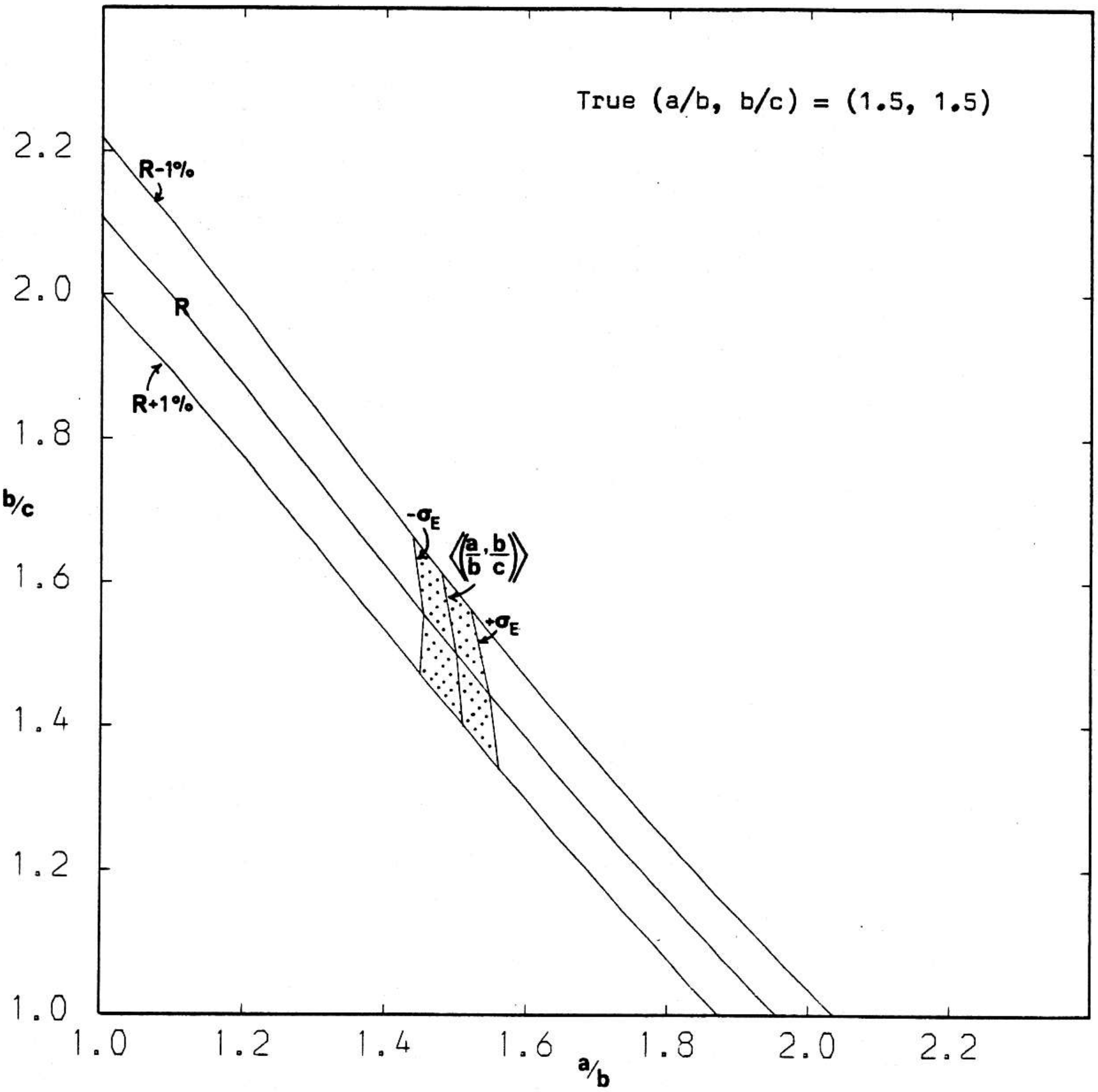

Figure 48. The area marked by dots represents the allowed band of retrieved axial ratios determined using the new R - constrained least squares algorithm for Protein 1. Simulated experimental error of ± 0.1° standard error on each data point for the electric birefringence decay curve was assumed.

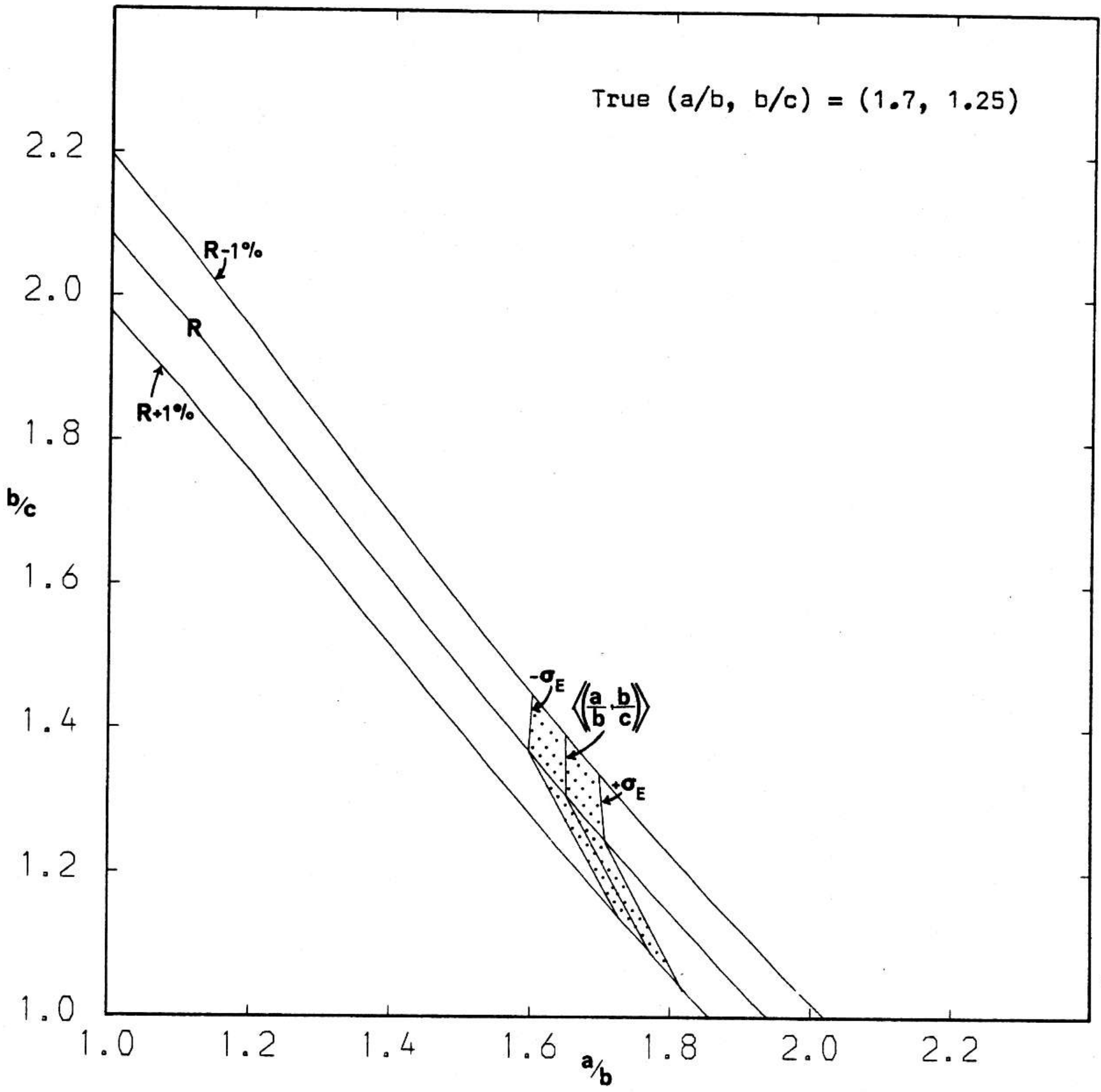

Figure 49. As for Figure 48 but for Protein 2

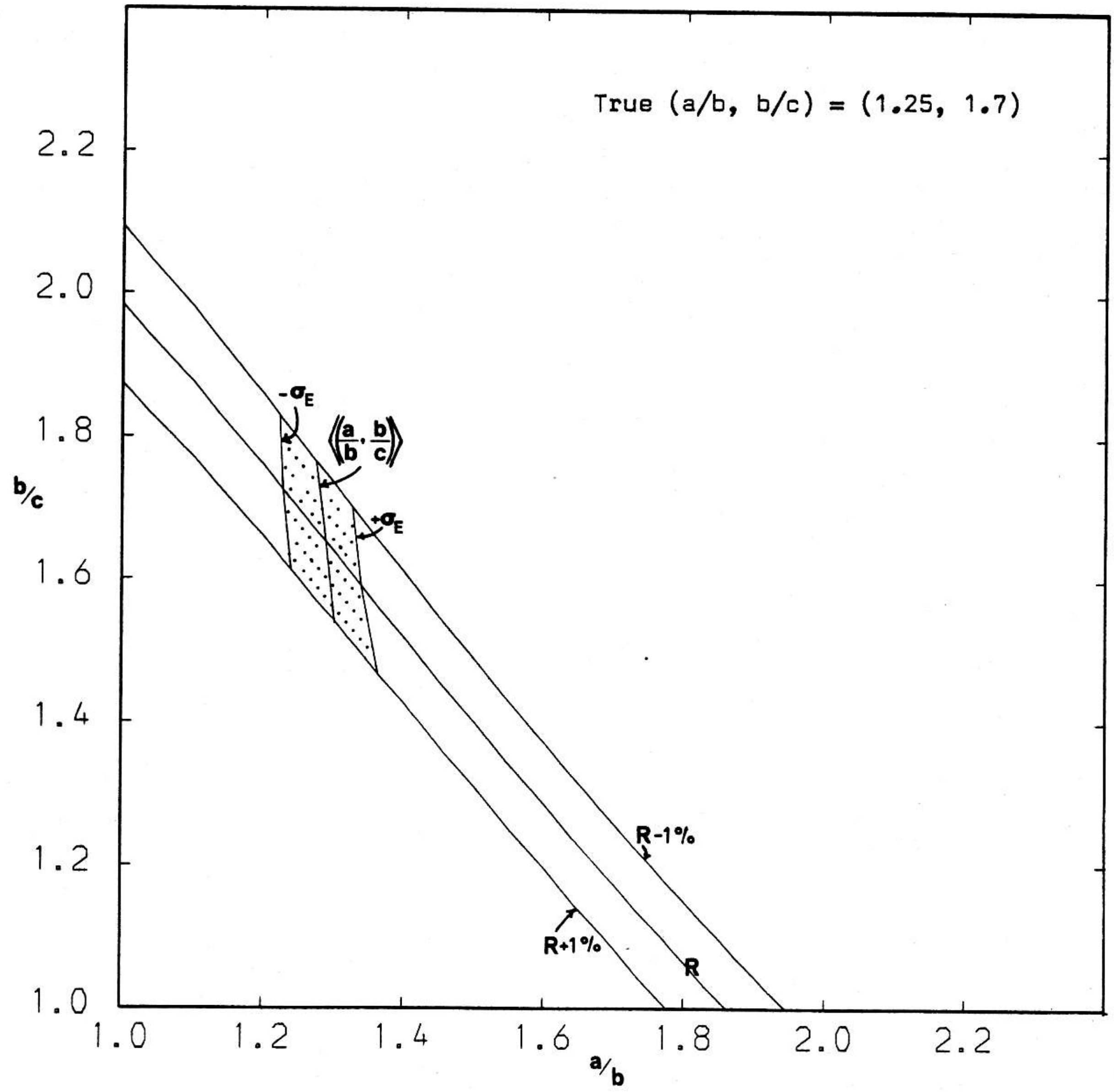

Figure 50. As for Figure 48 but for Protein 3

BIBLIOGRAPHY.

Alexander, A.E. and Johnson, P. (1949)
'*Colloid Science*', Volume 2, Oxford University Press

Alpert, S.S. and Banks, G. (1976)
Biophysical Chem. *4*, 287

Baghurst, P.A., Nichol, L.W., Ogston, A.G., Winzor, D.J. (1975)
Biochem. J. *147*, 575

Ballinger, K.W.A. and Jennings, B.R. (1979)
Nature *282*, 699

Batchelor, G.K. (1967)
'*An Introduction to Fluid Mechanics*', Cambridge University Press

Batchelor, G.K. (1970)
J. Fluid Mech. *41*, 545

Batchelor, G.K. and Green, J.T. (1972)
J. Fluid Mech. *56*, 375

Beeman, W.W., Koesberg, P., Anderegg, J.W. and Webb, M.B. (1957)
in '*Handbuck der Physik*', (Flugge, S. ed.), 32, 321, Springer-Verlagg (Berlin)

Benoit, H. (1951)
Ann. Physik. *6*, 561

Berne, P.J. and Pecora, R. (1974)
Ann. Rev. Phys. Chem. 25, 233

Blake, C.C.F. (1975)
Essays in Biochem. II, 37

Blake, C.C.F., Geisow, M.J. and Oatley, S.J. (1978)
J. Mol. Biol. 121, 339

Blake, C.C.F., Koenig, D.F., Mair, G.A., North, A.C.T., Phillips, D.C.
and Sarma, V.R. (1965)
Nature 206, 757

Bloomfield, V.A., Dalton, W.O. and Van Holde, K.E. (1967)
Biopolymers 5, 135

Bresler and Talmud (1944)
CR Acad. Sci. URSS, 43, 310

Brinkman, H.C., Hermans, J.J., Oosterhoff, L.J., Overbeek, J. Th. G.,
Polder, D., Staverman, A.J. and Wiebenga, E.H. (1949)
Proc. Int. Rheol. Congress (Schveningen) II, 77

Brenner, H. (1970)
J. Coll. Int. Sci. 32, 141

Brenner, H. (1972a)

Chem. Eng. Sci. 27, 1069

Brenner, H. (1972b)

Progr. Heat and Mass Transfer 5, 93

Cantor, C.R. and Tao, T. (1971)

Proc. Nucl. Acid Res. 2, 31

Cerf, R. and Scheraga, H.A. (1952)

Chem. Revs. 51, 185

Chapman, P.F. (1913)

Phil. Mag. 25, 475

Cheng, P.Y. and Schachman, H.K. (1955)

J. Polymer Sci. 16, 19

Chu, B. (1974)

'Laser Light Scattering', Academic, New York

Chwang, A.T. (1975)

J. Fluid Mech. 72, 17

Clenshaw, C.W. and Curtis, A.R. (1960)

Num. Math. 2, 197

Creeth, J.M. and Knight, C.G. (1965)
Biochim. Biophys. Acta 102, 549

Cummings, H.Z. and Pike, E.R. (1973)
(eds.) 'Photon Correlation and Light Beating Spectroscopy', Plenum, New York

Dickerson, R.E. and Geiss, I. (1969)
'The Structure and Action of Proteins', Benjamin, California

Dougherty, J. and Kreiger, I.M. (1972)
in Kreiger, Adv. Colloid Sci. 3, 111

Edsall, J.T. (1953)
in 'The Proteins' (Neurath, H. and Bailey, K. eds) 1B, Chapter 7, Academic, New York

Edwardes, D. (1892)
Quart. J. Math. 26, 70

Einstein, A. (1905)
Ann. Physik 17, 549

Einstein, A. (1906)
Ann. Physik 34, 591

Einstein, A. (1911)
Ann Physik 34, 591

Emes, C.H. (1977)
Ph. D. thesis, University of Leicester

Emes, C.H. and Rowe, A.J. (1978a)
Biochim. Biophys. Acta 537, 110

Emes, C.H. and Rowe, A.J. (1978b)
Biochim. Biophys. Acta 537, 125

Farrant, J.L. (1954)
Biochim. Biophys. Acta 13, 569

Feldman, R.J. (1976)
'Atlas of Macromolecular Structure on Microfiche', Traco Jitco Int., Rockville, Md. USA

Gans, R. (1928)
Ann. Physik 86, 628

Garcia Bernal, J.M. and Garcia de la Torre, J. (1980)
Biopolymers 19, 628

Garcia de la Torre, J. and Bloomfield, V.A. (1977a)
Biopolymers 16, 1747

Garcia de la Torre, J. and Bloomfield, V.A. (1977b)
Biopolymers 16, 1765

Garcia de la Torre, J. and Bloomfield, V.A. (1977c)

Biopolymers 16, 1779

Garcia de la Torre, J. and Bloomfield, V.A. (1978)

Biopolymers 17, 1605

Gardner, D.G., Gardner, J.C., Laush, G. and Meinke, W.W. (1959)

J. Chem. Phys. 31, 978

Giesekus, H. (1962)

Rheol. Acta 2, 50

Gill, P.E. and Murray, W. (1976)

Nat. Phys. Lab. report NAC 72

Gold, O. (1937)

Ph. D. thesis, University of Vienna

Goodwin, J.W. (1975)

Colloid Science 2 (Chemical Society), 246

Guoy, L.G. (1910)

J. Phys. Chem. 9, 457

Hall, C.E. and Slayter, H.S. (1959)

J. Biophys. Cytol. 5, 11

Harding, S.E. (1980a)
Biochem. J. 189 (in press)

Harding, S.E. (1980b)
mss. submitted to J. Phys. Chem.

Harrison, P.M. (1959)
J. Mol. Biol. 1, 69

Herzog, R.O., Illig, R. and Kudar, H. (1934)
Z. Phys. Chem. A167, 329

Holtzer, A. and Lowey, S. (1956)
J. Am. Chem. Soc. 78, 5954

Jablonski, A. (1961)
Naturforsch 169, 1

Jeffrey, G.B. (1922)
Proc. Roy. Soc. (London) A102, 476

Johnson, P. and Mihalyi, E. (1965)
Biochim. Biophys. Acta 102, 476

Jost, J.W. and O'Konski, C.T. (1978)
in 'Molecular Electro Optics' (O'Konski, C.T. ed.) Volume 2, 529

Kartha, G., Bello, J. and Harker, D. (1967)
Nature 213, 862

Kendrew, J.C., Bodo, G., Dintzis, H.M., Parrish, R.G., Wycoff, H. and Phillips, D.C. (1958)
Nature 181, 665

Kim, S.H. (1974)
in 'Biochemistry' (Stryer, L.) 653, Freeman, San Francisco

Kirkwood, J.G. (1967)
'Macromolecules' (Aueur, P.L. ed.), Gordon and Breach

Koenig, S.H. (1975)
Biopolymers 14, 2421

Kratky, O., Leopold, H. and Stabinger, H. (1969)
Z. Angew. Phys. 27, 273

Kratky, O., Leopold, H. and Stabinger, H. (1969)
in 'Methods in Enzymology' (Hirs, C.H.W. and Timasheff, S.N. eds.), 27, 98, Academic, London

Krause, S. and O'Konski, C.T. (1959)
J. Am. Chem. Soc. 81, 5082

Kuff, E.J. and Dalton, A.L. (1957)
J. Ultrastructure Res. 1, 62

Kuhn, W. and Kuhn, H. (1945)
Helvetica Chimica Acta 38, 97

Kynch, G.J. (1956)
Proc. Roy. Soc. (London) A237, 90

Labaw, L.W. and Wycoff, R.W.G. (1957)
Biochim. Biophys. Acta 25, 263

Lauffer, M.A. (1942)
Chem. Rev. 31, 561

Laurent, T.C. and Killander, J. (1964)
J. Chromatog. 14, 317

Lipscomb, W.N. (1971)
Proc. Robert A. Welch Found. Conf. Chem. Res. 15, 134

Lloyd, P.H. (1974)
'Optical Methods in Ultracentrifugation, Electrophoresis and Diffusion',
Clarendon Press, Oxford

Lucas, C.W. and Terrill, C.W. (1970)
Collected Algorithms from CACM, No. 404

Manley, R. and Mason, S. G. (1954)
Canad. J. Chem. 32, 763

Martin, R.B. (1964)
'Introduction to Biophysical Chemistry' Chap. 11, McGraw-Hill, New York

McCammon, J.A., Deutch, J.M. and Bloomfield, V.A. (1975)
Biopolymers 14, 2479

Mehl, J.W., Oncley, J.L. and Simha, R. (1940)
Science 92, 132

Mendelson, R. and Hartt, J. (1980)
EMBO Workshop on Muscle Contraction, Alpbach Conf. Austria

Mihalyi, E. and Godfrey, J. (1963)
Biochim. Biophys. Acta 67, 90

Memming, R. (1961)
Z. Physik. Chem. (Frankfurt) 28, 169

Mooney, M. (1951)
J. Coll. Sci. 6, 162

Mooney, M. (1957)
J. Coll. Sci. 12, 575

Munro, I., Pecht, I. and Stryer, L. (1979)
Proc. Nat. Acad. Sci. (USA) 76, 56

Nichol, L.W., Jeffrey, P.D., Turner, D.R. and Winzor, D.J. (1977)
J. Phys. Chem. 81, 776

Nisihara, T. and Doty, P. (1958)
Proc. Nat. Acad. Sci. (USA) 44, 411

Oberbeck, A. (1876)
J. reine. angew. Math. 81, 62

O'Connor, D.V., Ware, W.R. and Andre, J.C. (1979)
J. Phys. Chem. 83, 1333

Offer, G., Moos, C. and Starr, R. (1973)
J. Mol. Biol. 74, 653

O'Hara and Smith (1968)
Comp. Journal 11, 213

O'Konski, C.T. and Haltner, A.J. (1956)
J. Am. Chem. Soc. 78, 3604

Oliver, J. (1972)
Comp. Journal 15, 141

Oncley, J.L. (1940)
J. Phys. Chem. 44, 1103

Oncley, J.L. (1941)
Ann. New York Acad. Sci. 41, 121

Paradine, C.G. and Rivett, B.H.P. (1960)
'Statistical Methods for Technologists', English Universities Press, London

Pearce, T.C., Rowe, A.J. and Turnock, G. (1975)
J. Mol. Biol. 97, 193

Perrin, F. (1934)
J. Phys. Radium 5, 497

Perrin, F. (1936)
J. Phys. Radium 7, 1

Perutz, M.F., Rossmann, M.G., Cullis, A.F., Muirhead, H., Will, G. and North, A.C.T. (1960)
Nature 185, 416

Powell, D.R. and MacDonald, J.R. (1972)
Comp. Journal 15, 148

Pytkowickz, R.M. and O'Konski, C.T. (1959)
J. Am. Chem. Soc. 81, 5082

Rallison, J.M. (1978)
J. Fluid Mech. 84, 237

Riddiford, C.L. and Jennings, B.R. (1967)
Biopolymers 5, 757

Ridgeway, D. (1966)
J. Am. Chem. Soc. 88, 1104

Ridgeway, D. (1968)
J. Am. Chem. Soc. 90, 18

Rowe, A.J. (1977)
Biopolymers 16, 2595

Rowe, A.J. (1978)
Techniques in Protein and Enzyme Biochem. B105a, 1

Saito, N. (1951)
J. Phys. Soc. (Japan) 6, 297

Scheraga, H.A. (1955)
J. Chem. Phys. 23, 1526

Scheraga, H.A. (1961)
'Protein Structure', Academic, New York

Scheraga, H.A. and Mandelkern, L. (1953)
J. Am. Chem. Soc. 79, 179

Simha, R. (1940)

J. Phys. Chem. 44, 25

Simha, R. (1952)

J. Appl. Phys. 23, 1020

Shaw, D.J. (1970)

'Introduction to Colloid and Surface Chemistry' (2nd edn.), Butterworths

Small, E.W. and Isenberg, I. (1977)

Biopolymers 16, 1907

Sorenson, N.A. (1930)

CR Lab. Carlsberg 18, No. 5

Squire, P.G. (1970)

Biochim. Biophys. Acta 221, 425

Squire, P.G. (1978)

in 'Molecular Electro Optics' (O'Konski, C.T. ed.) Volume 2, 565

Squire, P.G., Moser, L. and O'Konski, C.T. (1968)

Biochemistry 7, 4261

Stacey, K.A. (1956)

'Light Scattering in Physical Chemistry', Butterworths, London

Stokes, Sir G. (1851)
Trans. Cambridge Phil. Soc. 9, 8

Stokes, Sir G. (1880)
'Mathematical and Physical Papers', Cambridge University Press

Svedberg, T. and Pedersen, K.O. (1940)
'The Ultracentrifuge', Oxford University Press

Tanford, C. (1955)
J. Phys. Chem. 59, 798

Tanford, C. (1961)
'Physical Chemistry of Macromolecules', Wiley, New York

Theorell, H. (1934)
Biochem. Z. 268, 46

Vand, V. (1948)
J. Phys. Coll. Chem. 52, 277

Van de Hulst, H.C. (1957)
'Light Scattering by Small Particles', Wiley, New York

Van Holde, K.E. (1971)
'Physical Biochemistry', Prentice Hall, New Jersey

Wahl, P. (1966)

Compt. Rend. Acad. Sci. (Paris) 263D 1525

Wales, M. and Van Holde, K.E. (1954)

J. Polymer Sci. 14, 81

Wilde, D.J. (1964)

'Optimum Seeking Methods', Prentice Hall, New Jersey

Williams, R.C., Ham, W.T. and Wright, A.K. (1976)

Anal. Biochem. 73, 52

Wilson, R.W. and Bloomfield, V.A. (1979a)

Biopolymers 18, 1205

Wilson, R.W. and Bloomfield, V.A. (1979b)

Biopolymers 18, 1543

Yang, J.T. (1961)

Adv. Protein Chem. 16, 323

Zimm, B.H. (1948)

J. Chem. Phys. 16, 1093

Zimm, B.H. (1956)

J. Chem. Phys. 24, 269